IMPACT AND FRACTURE TOUGHNESS PROPERTIES OF STRUCTURAL STEELS FOR DESIGN ENGINEERS

Prepared by:

Illinois Department of Transportation
Bureaus of Materials and Research
126 East Ash St.
Springfield IL 62704

February 2022

Technical Report Documentation Page

1. Report No.	2. Government Accession No.	3. Recipient's Catalog No.
PRR Number 174	N/A	N/A

4. Title and Subtitle

Impact and Fracture Toughness Properties of Structural Steels for Design Engineers

5. Report Date
February 2022

6. Performing Organization Code

8. Performing Organization Report No.

7. Author(s)
Christopher Hahin, MetE/MechE, CorrE, PE, Illinois Dept. of Transportation

8. Performing Organization Name and Address

Illinois Dept. of Transportation
Bureaus of Materials & Research
126 East Ash St.
Springfield, IL 62704

10. Work Unit (TRAIS)

11. Contract or Grant No.

13. Type of Report and Period Covered

Final Report, Jan 2020-Feb 2022

12. Sponsoring Agency Name and Address
Illinois Department of Transportation
Bureaus of Materials & Research
Springfield IL 62704

14. Sponsoring Agency Code

15. Supplementary Notes

16. Abstract

The energy absorption behavior of structural steels at a range of temperatures is important information to design, structural and materials engineers. Several historic examples of catastrophic failures which did not consider the energy absorption of steel at lower temperature are described. Impact toughness is related to fracture toughness, a quantifiable indicator that provides for prediction of safe conditions of structures subjected to stresses from static and cyclic loadings and impact loads. The general term structures includes bridges, piers, sign and signal structures, light poles, and barriers subject to impact, or any operating machinery associated with the structure. The influence of alloying elements in structural steels on transition temperatures and energy absorption are described in this report. Equations to predict impact transition temperatures and upper shelf impact energies based on chemical composition are proposed to aid in the pre-selection of steels that are appropriate for any low temperature operating conditions where the structures or their operating machinery are located. Accuracies of the equations were compared with actual transition temperatures and upper shelf energies in the technical literature. Several equations to convert Charpy V-notch impact toughness into fracture toughness are also provided to evaluate effects of stresses, impact loads and crack sizes with respect to the safety and durability of the structure or its operating machinery.

17. Key Words	18. Distribution Statement
Transition temperature; impact toughness; upper shelf energy; Charpy V-notch test; fracture toughness; chemical composition; alloying elements; prediction equations.	Unlimited.

19. Security Classif. (of this report)	20. Security Classif. (of this page)	21. No. of Pages	22. Price
Unclassified	Unclassifed	65	

Form DOT F 1700.7 (8-72) Reproduction of completed page authorized

TABLE OF CONTENTS

LIST OF TABLES AND FIGURES

IMPACT AND FRACTURE TOUGHNESS PROPERTIES OF STRUCTURAL STEELS FOR DESIGN ENGINEERS

Introduction

Numerous examples of structural and ship steels under conditions of impact or ambient stress when cracks were present that sustained partial fracture or complete rupture have been widely studied. These include the splitting apart or extensive damage that Liberty Ships sustained in colder weather during World War 2, the catastrophic collapse of the Silver Bridge in Ohio due to stressed eyebars made of high carbon steel, and the sinking of the Titanic due to rupture of hull plates and rivets when it struck an iceberg in the North Atlantic. This report addresses hot rolled and normalized structural steels whose carbon contents can range up to 0.80%, but principally concentrates on structural carbon and alloy steels generally limited to 0.40% carbon.

Of the 2,708 Liberty Ships produced, 1,031 sustained severe damage, split or sunk due to a low impact toughness of 15 ft-lbs for ship plate steels (Harris and Williams, 1956), in a temperature range of 2º-21°C (35-70°F), a transition temperature range of 27º-43°C (80º-110°F), with an average impact toughness of 54 joules (40 ft-lbs). At the transition temperature, the fracture surface is 50% ductile.

A high yield or tensile strength steel, depending on its composition and alloy content, may not be appropriate if it has a high transition temperature and low fracture toughness. The bridge eyebar in the Silver Bridge failure in West Virginia was an SAE 1060 carbon steel that had a typical tensile strength of 840 MPa (122 ksi) and yield strength of 605 MPa (88 ksi). However, its typical CVN impact toughness at 0ºC (32°F) was only 3 joules (2 ft-lbs) and had a transition temperature of 90ºC (194°F). At 24ºC (75°F), its Charpy V-notch toughness was only 3-7 joules (2-5 ft-lbs). At 7 joules (5 ft-lbs), this translates to a low fracture toughness of only 27 MPa $[m]^{0.5}$ (25 ksi $[in]^{0.5}$). At 50% of its yield strength at 305 MPa (44 ksi), a critical crack length for that eye bar was only 2 mm (0.084 in), which is barely visible to the unaided eye. Moreover, cracks were obscured by the presence of rust at the eyebar-pin connections during inspections (National Transportation Safety Board, 1970).

In the case of the Titanic, its hull plates had a transition temperature of +50°C (104°F) and its impact energy at 0°C (32°F) was only 4 J transverse (3 ft-lbs) and 24 J longitudinal (18 ft-lbs), clearly unsuitable for collision with an iceberg three times its size (Foecke, 1998).

In each of these cases of catastrophic failure, temperature, applied stresses, notches and composition of the steel produced the right conditions for steel to enter the ductile-to-brittle transition zone. In this report, the relationship of energy absorption, composition and selection of the appropriate impact toughness requirements for structural steels that are subject to rapid or impact loading in locations with specific operating or service temperatures, are thoroughly described.

Importance of Impact and Fracture Toughness and Temperature in Structural Design

Various types of common structures are subject to impact forces, including but not limited to: (a) critical load-carrying members of bridges and any operating machinery; (b) light poles; (c) sign and signal structures; (d) anchor bolts, guardrails and barriers; (d) piers of bridges and their protection cells; (e) locks and dams; (f) port facility wharves; and (g) security walls and barriers. These structures are typically subjected to static dead loads, fatigue stresses due to live loads, and variable impact loads. Some are exposed to variable wind loadings.

Impact load forces may be derived from moving loads from trucks or automobiles, river barges, dropped weights, cranes, explosions or pressure vessel blasts, major electric arc discharges or tectonic-seismic events. Strain rates can vary from intermediate to very fast, depending on the speed of impact of the load. Trucks routinely weigh 36,290 kg (80,000 lbs) or more and travel at 70 mph (103 ft/sec/31 m/sec), which far exceeds the very slow strain rate used in a standard tensile test and 6 times greater than the impact velocity of the Charpy V-notch test at 16 ft/sec or the dynamic tear test. The release of high-pressure gas can range from 50-200 ft/sec and pressure wave velocities from explosions of gas or fuel mixtures range from 1000 to 8000 ft/sec (Wilson, 1964).

The energy absorption response of steel under impact conditions can be measured by several tests. The most widely used tests are the Charpy V-notch test (ASTM E23), the dynamic tear test (ASTM E604) and the drop weight test (ASTM E436). Each of these tests have correlation to fracture toughness, a value obtained under slow-strain rate conditions. Fracture toughness is a material property that indicates tolerance to fracture when a material is cracked and is subject to tensile or bending stresses.

Shape of the Impact Energy Absorption Curve for Ferritic Structural Steels

The impact absorption energy curve for iron and steels is S-shaped and are shown in *Figure 1* and *Figure 2* of this report. The transition temperature is the point of inflection where the energy changes from a higher ductile energy absorption down to substantially brittle energy absorption. Where this transition temperature is located on the absorption curve is particularly important when choosing a material that has high fracture toughness at the lowest service temperatures that any structure will encounter or where its machinery will operate.

In general, the change in impact energy absorption in steels and where this occurs at specific temperatures is strongly influenced by the carbon, sulfur and phosphorus contents of the particular steel and the presence of other minor alloying elements. The behavior of steels under stress that are affected by impact forces and have substantial dead and live loads applied at subfreezing temperatures is an important consideration that must be taken into account when designing any structure or mechanical system.

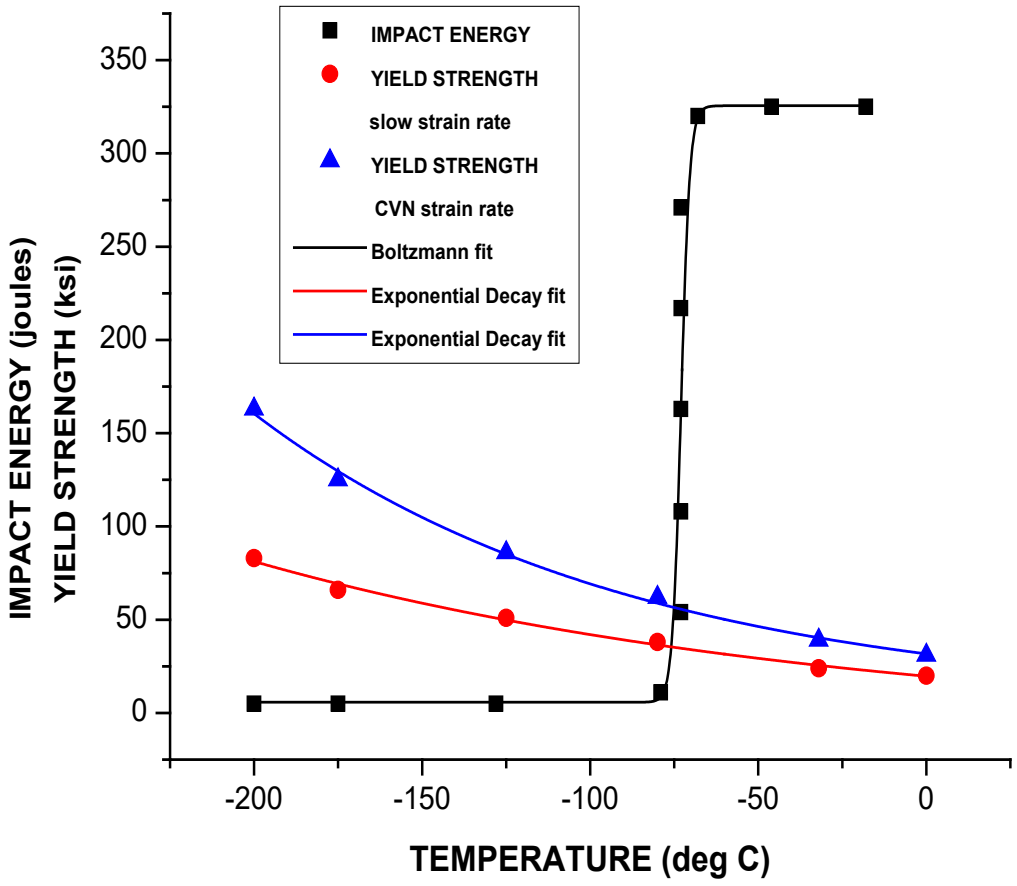

Figure 1. The impact energy absorption of commercially pure iron compared to its yield strength at a range of temperatures. As temperatures decrease, the yield strength of iron at slow strain rates increases, but substantially increases at higher strain rates. Commercially pure iron contains 0.01% carbon and at approximately -70°C the lower shelf is established. The transition temperature range for commercially pure iron is approximately -70° to -75°C, depending on the presence of residual impurities. Impact energy absorption for iron as a function of temperature is S-shaped (sigmoidal fit) and its yield strength at cryogenic temperatures is an exponential decay fit. The upper shelf has an impact energy absorption level of 300-325 joules and the lower shelf only 5 joules (3.7 ft-lbs). For pure iron, the transition temperature region is very narrow and sharply defined, but its vertical theta angle of 2-4°, Θ as described in *Figure 2*, substantially increases as carbon content increases, as shown in *Figure 3*.

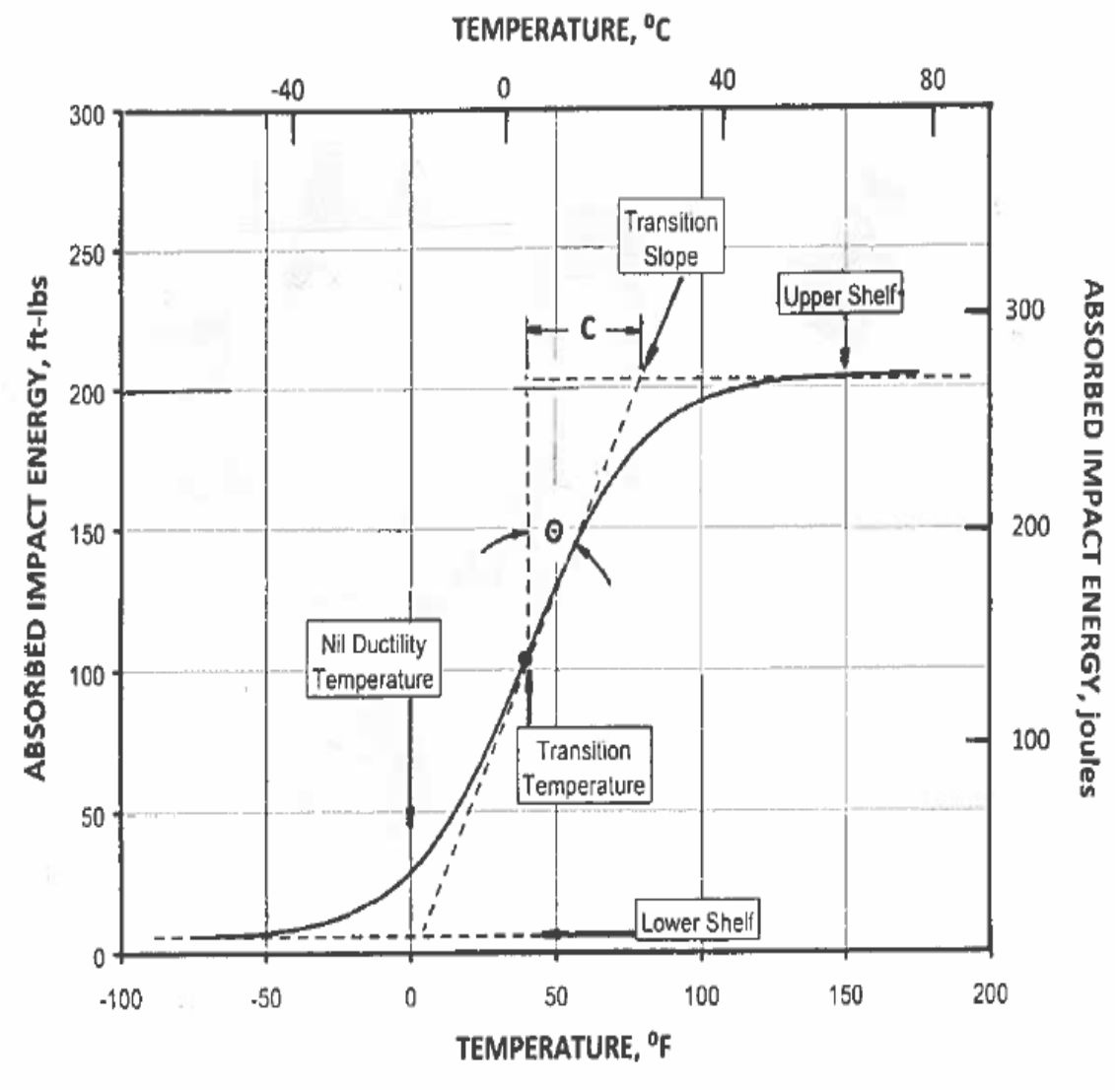

Figure 2. The principal generic elements of a ductile-to-brittle energy vs. temperature curve for steels with a body-centered cubic structure consists of a lower shelf with minimal impact energy absorption; a transition zone whose slope is characterized by the transition angle theta; and the upper shelf which absorbs the greatest amount of energy. The transition temperature is located where the average energy value, ½ [upper shelf energy + lower shelf energy], intersects the temperature axis.

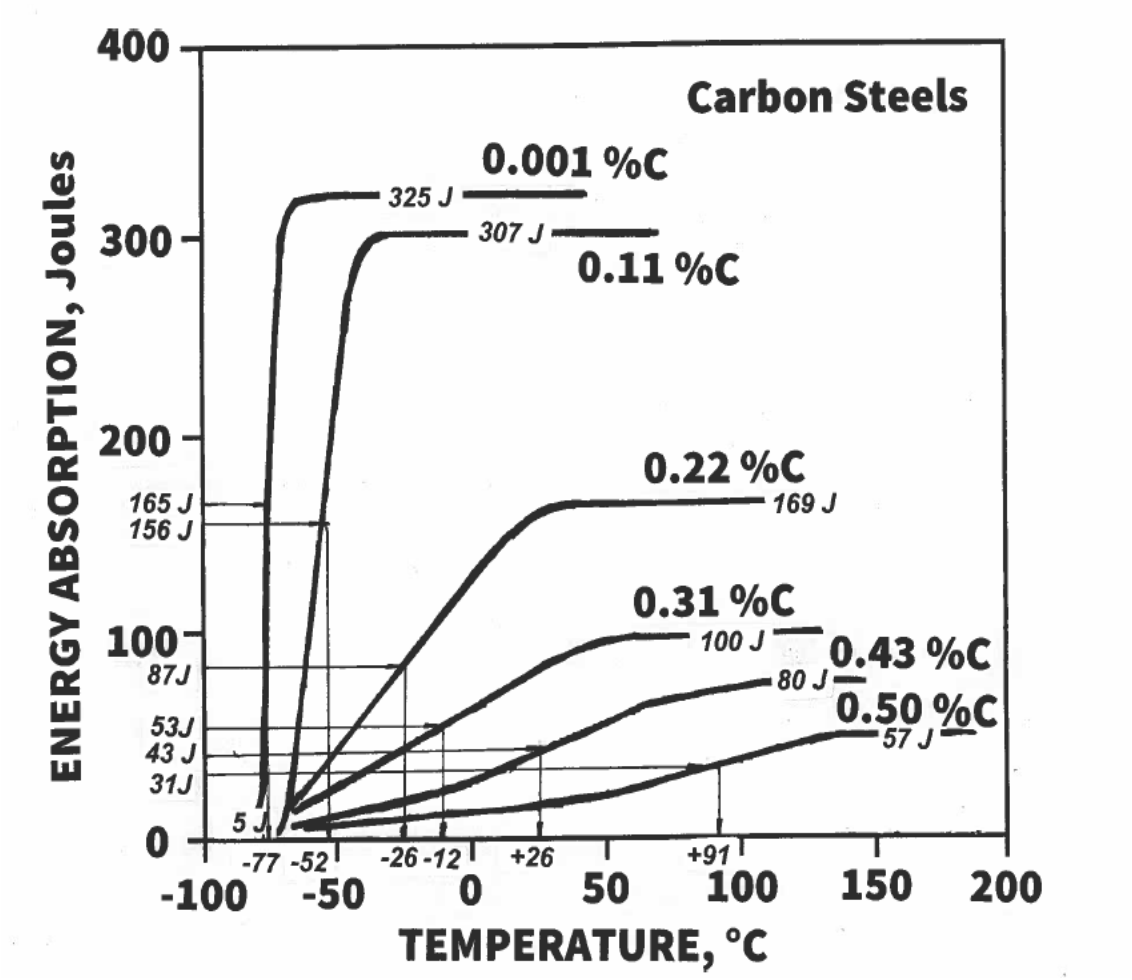

Figure 3. This is a generic plot of the impact energy absorption vs. temperature for various carbon steels as a function of carbon content. The transition temperature is determined by plotting the upper shelf and lower shelf energies of the tested steel and all test values in between on the ordinate and their respective test temperatures on the abscissa. The average of the [upper shelf energy + lower shelf energy] ÷ 2 is calculated and extended to where the average energy intersects the plotted curve. That point of curve intersection with average energy corresponds to the transition temperature on the abscissa. Because various elements besides carbon like manganese, nickel, vanadium, sulfur and phosphorus can significantly affect transition temperature, this diagram is not intended to represent transition temperatures for all carbon and alloy steels in general. Each steel must be tested due to inherent compositional differences. For older steels and ASTM A36, the knowledge of silicon contents and thickness are quite significant when determining transition temperature; otherwise lower transition temperatures will be obtained from calculated estimates rather than actual higher values.

The transition temperatures of ferritic (magnetic) steels are increased by the elements carbon, sulfur, phosphorus and silicon, as shown in the following table for the ranges of their contents normally found in commercial structural steels. The other commonly used alloying elements, consisting of nickel, molybdenum, vanadium, niobium and aluminum, decrease the transition temperature.

The upper shelf of pure iron is decreased from approximately 300 to 325 joules of energy absorption by the elements carbon, sulfur, phosphorus, silicon, chromium, molybdenum, and copper. Copper will depress the upper shelf if the steel does not contain a nickel addition that is at least 50% of the copper content. This level of nickel will increase the solubility of copper in austenite, limiting the precipitation of copper in the grain boundaries when the steel is rolled and cooled to ambient temperatures. Manganese will raise the upper shelf energy. The effects of various elements on transition temperature and upper shelf energy, in their typical ranges found in commonly used structural and machinery steels, are summarized in *Table 1*.

Table 1. General Effects of Alloying Elements on Structural and Machinery Steels

Element	*Typical Range*	*Effect on Transition Temperature, °C*	*Effect on Upper Shelf Energy, joules*
Carbon	0.01 - 0.50	Increases 31° for every 0.1%	Decreases 150 J from 0.0% to 0.20%; decreases about 40 J for every 0.1% above 0.20%
Manganese	0.4 - 1.90	Decreases 5° for every 0.1%	Increases 1.1 J for every 0.1%
Sulfur	0.01 - 0.05	Increases 7° for every 0.1%	Decreases 15 J for every 0.01%
Phosphorus	0.01 - 0.05	Increases 8° for every 0.01%	Decreases 4 J for every 0.01%
Silicon	0.3 - 2.2	Increases 7° for every 0.1%	Decreases 3 J for every 0.1%
Nickel	0.0 - 2.00	Decreases 1.3° for every 0.1%	Relatively neutral
Copper	0.0 - 1.00	Increases 1.2° for every 0.1%	Decreases 2 J for every 0.1%
Vanadium	0.0 - 0.15	Decreases 11° for every 0.1%	Relatively neutral
Molybdenum	0.0 - 0.40	Decreases 15° for every 0.1%	Decreases 7 J for every 0.1%
Niobium	0.0 - 0.03	Decreases 10° for every 0.1%	Relatively neutral
Chromium	0.0 to 0.9	Relatively neutral	Decreases 2 J for every 0.1%

Any steel selected by the design engineer needs to be evaluated for its lowest mean anticipated service temperature (LMAST), its peak stresses sustained by live and dead loads, including impact loads, and the required transition temperature and upper shelf energy. Estimates of transition temperature and upper shelf energy can be obtained from the following predictive equations whose derivations are described in the technical supporting analysis Appendix of this report.

Prediction of Transition Temperature and Upper Shelf Energy from Composition

The transition temperatures and upper shelf energies determined from the chemical compositions of hot-rolled structural and machinery steels can be taken from: (a) preferably from actual heat compositions provided by the steel manufacturers or suppliers; (b) product analysis of plates, tubing or structural components obtained by laboratory analysis of steels in inventory or directly intended for use; or (c) nominal compositions of the alloys to be selected. Because Charpy test data has variations, the accuracy of the transition temperatures and upper shelf energies obtained by the prediction equations were compared with actual energy absorption curves taken from the published technical literature.

To estimate transition temperature for hot-rolled structural steels from composition, the prediction equation is:

$$T_{CVN} = -70 + 311(\%C) - 53(\%Mn) + 780(\%P) + 74(\%S) + 69(\%Si) - 13(\%Ni) + 12(\%Cu) + 145(\%Mo) - 106(\%V) - 102(\%Nb) - 170\ (\%Al) + 0.9(t - 13)$$

where T_{CVN} = Charpy V-notch transition temperature, ºC

t = thickness, mm

This equation has an accuracy of 1.2°± 9°C, and all percentages are in weight percent. Actual weight percentages of each element are to be taken from certified heat or product analysis of the steels intended or furnished for the construction project.

To determine the upper shelf energy, the prediction equation is:

$$E_{USE} = 3 + 307\ e^{-[(\%C - 0.0194)\ /\ 0.294]} + 11\ (\%Mn) - 1456\ (\%S) - 390\ (\%P) - 30\ (\%Si) - 16\ (\%Cr) - 24\ (\%Cu) - 72\ (\%Mo)$$

Where E_{USE} = upper shelf energy, joules

This equation has an accuracy of -0.6 ± 10.3 joules and a 3.1 ± 4.0% error with respect to total upper shelf energy.

If the transition temperature of the steel is determined to be questionable or may be unsuitable for the intended location of the structure, or that the upper shelf energy indicates insufficient impact toughness for the live and dead loads applied to the structure, the alloy selected by the designer should be tested before it is specified. If the specific steel selected or furnished is still unsuitable after testing, then other alloys with better toughness must be considered and tested before any alloy specification is finalized for use in specific project plans.

Correlation of Impact Notch Toughness with Fracture Toughness

The combined effects of impact loads from trucks and passenger cars, fatigue and dead load stresses on bridge members, sign and signal structures, piers, abutments, and supporting concrete, can result in substantial damage or even collapse of the structure or its operating machinery. The cost of a Charpy V-notch (CVN) test is substantially less than a fracture toughness test and is more suited to test sections of members of various sizes and thickness. Subsize CVN specimens must be 3 mm (0.125 in) thick, but their test results must be adjusted to comparable standard-size impact test bars which are 10 x 10 x 55 mm in dimension. The impact toughness values obtained from calculation and testing can then be translated into fracture toughness by various conversion equations.

Fracture toughness K_{Ic} or K_{mat} is a material property and is expressed in the following form:

$$K_{Ic} = C\,\sigma\,[\pi\,a]^{0.5}$$

Where K_{Ic} = fracture toughness in tension

C = geometry of the developed crack and where the stresses are applied

a = critical crack size or depth

σ = applied nominal stress determined from dead + live loads

If applied stress is magnified by stress concentration factors, magnified stress should be used.

A conversion of CVN impact energy to fracture toughness that is not dependent on strain rate is the Roberts-Newton equation, $K_{Ic} = 9.35\,[CVN]^{0.63}$, which is used for conversion of impact toughness to fracture toughness for medium-to-higher strength steels (CVN is in ft-lbs). The Barsom-Rolfe conversion equation, $K_{Id} = [5\,CVN \times E]^{0.5}$, uses pre-cracked CVN specimens and can represent dynamic energy absorption conditions of impacted members that have fatigue cracks. An alternate equation to determine K_{Id} without pre-cracking is the Corten-Sailors equation, $K_{Id} = 14.6 \times [CVN]^{0.5}$. There are several other CVN to K_{Ic} conversion equations listed in the supporting analysis Appendix of this report.

Lowest Anticipated Mean Service Temperature

Location will determine the service temperatures in which the structure will function, or what are the operating temperature ranges of any of its exposed machinery. These temperatures can widely vary, particularly where winter temperatures frequently dip below freezing for several months. It is at these lower temperatures where structural and machinery steels are most vulnerable to losses of impact energy absorption and fracture toughness.

Daily records of temperature changes are kept for both large and medium sized airports by the National Weather Service. Use of these records provide reasonably accurate data of daily colder temperatures. Airports that are in the closest general vicinity of the structure within Illinois or any of its neighboring states can provide accurate accounts of temperature variations, especially for the colder months of the year. A general depiction of temperature variations in the northern, central and southern parts of Illinois is provided in *Table 2* which lists the average (mean) low temperatures and their standard deviations for the three coldest months of the year for Chicago, Springfield and St. Louis, MO. Data was obtained from the National Weather Service over a 100 year period from 1921 to 2021. Chicago reflects the colder temperatures of the northern portion of the Illinois; temperatures recorded at the Springfield airport are intended reflect the central portion of the state, and the weather records of St. Louis represent the southern portion. *Table 2* also indicates a mild effect of latitude on low temperature variations. The methodology presented here to determine the lowest mean anticipated service temperature (LMAST) can apply to any city or regional airport in any state or country.

Table 2. Mean Low Temperatures and Standard Deviations for the Coldest Months, 1921-2021

City	*December*	*January*	*February*
Chicago	1.9°F ± 12.1°	-5.0°F ± 13.5°	-0.14°F ± 8.5
Springfield	0.44°F ± 9.1°	-3.8°F ± 9.3°	0.71°F ± 11.9
St. Louis, MO	7.6°F ± 8.5°	1.7°F ± 8.8°	7.2°F ± 8.5°

Lowest Mean Anticipated Service Temperature and Acceptance of Steels

First an estimate of the transition temperature is determined by the prediction equation, which is based on the composition of the steel. It is intended that the LMAST should be greater than the transition temperature so that the CVN energy of the structural steel will be preferably in or near the upper shelf region. If the impact toughness of the steel is not in the upper shelf at the LMAST, but

is in the transition region, the fracture toughness of the steel can still be predicted by the previously cited conversion equations, or the conversions listed in the technical analysis of the Appendix that supports this report.

After converting CVN energy to fracture toughness, the K_{Ic} or K_{Id} obtained should be enough to provide sufficient longevity, durability, or survivability of the structure when it sustains stresses, due to a combination of dead and live loadings and various impact forces, that would generate fatigue cracks. The size and location of these cracks under stress at the lowest anticipated service temperatures can determine the safety and durability of the structure. Crack sizes can be determined by periodic inspections and prior history of any crack propagation and knowledge of vulnerable design details. If the calculated transition temperature or the position of the upper shelf and the derived fracture toughness are at variance with mill or service center reports of impact toughness, then the steel should be tested to evaluate its actual impact toughness as a function of temperature. If the steel is still questionable or undesirable, it should be rejected prior to acceptance, and then another steel with better properties at lower temperatures can be selected.

Conclusions and Recommendations

Structural and machinery steels have impact notch toughness and fracture toughness properties that are subject to changes in temperature. At very low temperatures, they exhibit “brittle” behavior where energy absorption is limited to 5-7 joules (4-5 ft-lbs). As temperatures increase, their impact notch toughness values also increase in the transition zone. The S-shaped energy absorption curves for various steels vs. temperature are altered by the presence of certain elements. As temperatures further increase, the maximum energy absorbed by the steel forms a plateau called the upper shelf, which is generally more ductile and impact energy absorptive.

The elements that markedly shift the position and tilt of the transition zone and decrease the upper shelf energy are carbon, phosphorus and sulfur. Other minor alloying elements can also increase or decrease the transition temperature, which is an inflection point that lies between the lower and upper shelf energy that intersects the temperature axis of the energy absorption curve.

Equations which predict the transition temperature and the upper shelf energy as a function of steel composition were developed and presented in this report. The accuracy of the transition temperature prediction equation is within 1.2° ± 9.0°C. The accuracy of the upper shelf prediction equation is -6.1 ± 6.8 joules, which is within -3.1 ± 4.0% of the total upper shelf energy.

Considering the variations of CVN data, these prediction equations are quite accurate. A variation of 2/3 of the minimum required impact toughness is permitted by ASTM A370 is considered acceptable. Transition temperatures for commonly specified structural steels range from -94° to +8°C. Typical upper shelf energies for common structural steels range from 140 to 275 joules. The origin and influences of composition on the S-shaped ductile-to-brittle transition curve are thoroughly described in a supporting technical analysis Appendix of this report.

Low temperature variations throughout northern, central and southern Illinois from 1921 to 2021 were represented by official National Weather Service records from Chicago, Springfield and adjacent St. Louis MO to show effect of latitude and location in the three coldest months of the year. Using mean low temperatures and standard deviations for the three coldest months from nearby airports where the project will be located will provide a general representation of temperature variations that the structure, and if applicable its operating machinery, will encounter during the intended service life.

From the general temperature environment, especially during the coldest months, the transition temperature and upper shelf energy can be estimated for the steels selected for use. It is strongly recommended that whichever steels are selected that actual energy absorption tests be conducted before final specification for project construction or rehabilitation. This will confirm the estimation and provide greater confidence to the project designer that the steels selected will provide structural reliability under the influence of impact, live and dead stresses that the structure or operating machinery could or will encounter during its intended design life.

It is most desirable that the selected steel should operate near or in the upper shelf zone at the lowest anticipated service temperature. The ordering of steel with a specific composition may not be practical due to a variety of factors, including availability, price and delivery time. The equations which predict transition temperature and upper shelf energy are useful because they permit the user to determine in advance whether the steel, based on its certified heat or product analysis, is suitable for the construction project and its location. Property estimates should always be verified by certified physical tests of energy absorption over the expected service range of temperature. Steels with very low levels of sulfur, carbon and phosphorus often come at a premium and may involve special orders. However, if the structure has a high probability of being impacted or is subject to fatigue cracking and operates at sub-freezing temperatures, the safety and long term service of the structure should take precedence over product acquisition time or cost.

APPENDIX

This appendix provides the fundamental technical analysis for this report and the basis for its recommendations and conclusions. The analysis references the technical literature and results of extensive research work done on the problem of ductile-to-brittle transition temperatures in steel alloys since the end of World War II to the present day.

Theoretical and Historical Basis of Impact Energy Absorption in Ferritic Steels

The velocity of transfer of impact loads can generate stresses through various materials is governed by their density and modulus of elasticity by the relationships for uniform beams, slabs, plates and cylinders (Wasley, 1973; Blake, 1990):

$$C = (E \div \rho])^{0.5} \text{ for uniform beams}$$

$$C = (E \div [(1 - v^2) \times \rho])^{0.5} \text{ for slabs, plates and cylinders}$$

Where C = sonic velocity in fps [m/sec]
E = modulus of elasticity, psi [MPa]
v = Poisson's ratio, typically 0.3 for steel
ρ = mass density, [wt /vol] / g
g = acceleration of gravity, 386.4 ft/sec^2 [117 m/s^2]

For steel, stress waves travel in plates at a velocity of 17,650 fps. For concrete, based on its lesser density of 155 lbs/ft^3, the stress wave velocity is reduced to 10,738 fps.

The dynamic impulse stress σ_0 resulting from an impact velocity is $\sigma_0 = V (E \times \rho)^{0.5}$, where V is the initial impact velocity (Blake, 1990). For a structural steel with a yield strength of 345 MPa (50 ksi) sustaining an impact velocity at 30.5 m/s (100 ft/sec), elastic contact stress is 1234 MPa (178 ksii, clearly above its yield strength. However, high strain rates raise the yield strength of steel. This contact stress is a theoretical elastic stress, where the material actually yields and undergoes plastic deformation and absorbs a portion of this energy. Impact energy applied to a steel with a yield strength of 345 MPa (50 ksi) results in energy absorption by both elastic and plastic deformation. The remaining portion of impact energy is sent as an impact stress wave and travels through the structure. The impact wave is also subject to impedance attenuation due to

metal grain sizes and any interface transfer of the stress wave to other materials such as concrete, rubber or plastic.

The energy absorption response of steel under impact conditions can be measured by a variety of tests. The most widely used tests are the Charpy V-notch test (ASTM E 23), the dynamic tear test (ASTM E604), and the drop weight tear test (ASTM E 436). Each of these tests have correlations to fracture toughness, a value obtained under slow-strain rate conditions. Fracture toughness is a material property that indicates tolerance to fracture when a material is cracked and is subject to conditions of tensile or bending stress.

Formation and Origin of the Brittle-to-Ductile Transition in Steel

Commercially pure iron exhibits a very sharp transition between ductile and brittle behavior that is a function of temperature, whereby the energy absorbed under impact conditions goes from being very limited to very substantial in a relatively short range of temperature. The transition temperature is typically measured as the point of inflection of a sigmoidally-shaped curve. The nil-ductility temperature is chosen at the bottom of the curve where brittleness dominates the fracture behavior. The lower shelf typically has an energy absorption of 5-7 joules compared to 330 joules or more for the upper shelf.

Early work before World War II demonstrated the strong temperature dependence of the impact toughness of commercially pure iron (Epstein, 1932), but the ductile-to-brittle behavior of steel was more vigorously studied after the catastrophic fractures of Liberty Ships produced during World War II. After the conclusion of the war, seminal research work was begun on trying to understand the mechanisms and causes of the ductile-to-brittle transition in carbon and alloy steels. The effects of each significant alloying element used in the production of iron-carbon alloys on notch toughness were examined by various research laboratories by impact testing alloys of virtually equivalent composition, except that the concentrations of each alloying element were varied and their effects on transition temperatures were measured (Reinbolt and Harris, 1951; Hoyt, 1952; Burns and Pickering, 1964; Vishnevsky and Steigerwald, 1968). Efforts to understand these iron-carbon alloy interactions, temperature and strain rate continue to the present day.

Figure A1 shows the sharp transition for current-day commercially pure iron for Charpy impact toughness using a V-shaped notch with a sharp tip radius of 0.25 mm. Initial work by Epstein in 1932 to measure the transition temperature for commercially pure irons that contained trace levels

of interstitial elements had a transition temperature range of -60º to -40ºC. When extrapolated to a theoretically “pure iron” without the presence of any trace elements, the transition temperature is -70ºC. Although the plot of *Figure A1* is fitted to a Boltzmann distribution function, it can also be expressed as a hyperbolic tangent function (Pluvinage, Capelle, Azari, Furtado, and Jallais, 2013).

From the freezing point of water down to -200ºC, the yield strength of commercially pure iron markedly increases in comparison with its impact energy absorption, as shown in *Figure A1.* As the yield strength of pure iron decreases, there is a rapid change in the amount of impact energy absorbed at about -70ºC, sharply rising from its lower shelf and leveling off to an upper shelf at -60ºC. This jump in impact energy absorption is called the ductile-to-brittle transition region. The point of inflection on the sigmoidal curve for pure iron is located in a narrow range of about -75° to -70ºC, depending on the presence of trace levels of interstitial elements. Simultaneously, the yield strength of iron substantially increases as temperatures decrease to cryogenic levels. In the upper shelf region, the impact toughness of commercially pure iron above 100ºC eventually begins to gradually decrease by exponential decay due to decreases in yield and tensile strength up to 500ºC.

The reasons why the strength of iron increases as temperature decreases can be explained on an atomic basis. The crystal structure of iron is body-centered cubic (bcc), whereas more ductile metals like aluminum and copper are face-centered cubic (fcc). Iron and its alloys in commercial form have a polycrystalline grain structure whereby each grain has a different orientation of its bcc crystal structure. Alloys with an fcc structure have a larger number of planes of higher atomic density than bcc crystal structures. The bcc structure has 32% of empty space compared to only 26% for the fcc structure (Andrews and Kokes, 1963). The bcc structure has fewer planes of higher atomic density in which plastic deformation can occur in comparison to the fcc structure. In these spaces of lesser packing, smaller interstitial atoms of alloying elements like carbon, phosphorus and nitrogen can position themselves, distorting the bcc crystal structure. *Figure A2* shows the adverse effect of carbon content on the shape and amount of energy absorbed in carbon steels. In pure metals, the bcc crystal structure, even without any interstitial elements being present, is still not perfect, but contains vacancies and crystal structure imperfections and defects called edge, screw and mixed dislocations. The bcc structure anomalies along these planes of atomic density lead to a process called slip or glide when applied stresses are beyond the yield strength. It is

estimated that there may be as many as 10^8 dislocations per cm^2, and even more after the metal is cold worked (Hume-Rothery and Raynor, 1962).

Dislocations can be annihilated by the presence of vacancies or actual voids in the bcc structure. Vacancies are created by the vibration of atoms due to their thermal excitation. As temperature increases, the number of vacancies increases by a thermally activated Arrhenius process (Reed-Hill, 1964):

$$n_v / n_o = e^{-Q/kT},$$

where n_v = number of vacancies
n_o = number atoms
Q = activation energy
k = Boltzmann constant
T = temperature, ºK

For pure polycrystalline iron, Q/kT is about 21.8, whereas the average for bcc metals is 25.0 (Giannattasio, et. al., 2010). The ratio of vacancies to number of atoms is very small, on the order of 3.4×10^{-10}, but this ratio still provides sufficient space for small atoms to fill these vacancies or lock down the number of dislocations which can impede plastic deformation (Reed-Hill, 1964). When iron is exposed to decreasing lower temperatures, the motion of these dislocations is substantially attenuated because the energy for activation of plastic deformation is reduced. In addition, the overall bcc crystal structure itself restricts the amount of plastic deformation. The deformation process at these cold temperatures then becomes largely elastic, whereby the iron fractures by cleavage separation along the planes of atomic density which are fewer than those in metals that have a face centered cubic structure. Deformation along the planes of atomic density that contain dislocations and vacancies may also have interstitial solutes present like carbon, sulfur or phosphorus atoms. These interstitial atoms are impediments to plastic deformation of iron under tensile or compressive loads that would exceed its yield strength.

Steels are composed of iron alloyed with other elements, resulting in changes to the mechanical properties of iron. Elements which have approximately the same size as the iron atom are termed substitutional solids. Although they often typically increase yield and tensile strength, they do not distort the bcc crystal structure of iron as much as the interstitial solids like carbon, sulfur or phosphorus due to their tendency to form interstitial compounds. Most of the alloying elements which have similar atomic radii as iron tend to decrease the transition temperature of steel. Their

similar or increased size tends to fill spaces that could be potentially be occupied by interstitials. Moreover, many of these elements are “austenite formers”, tending to create greater atomic packing than the bcc lattice would accommodate. See *Figure A3* which shows this relationship between the % of atomic radius of iron vs. radii of other alloying elements and how the transition temperature is either increased or decreased. Interstitials and their tendency to bind with other elements not only distort the bcc crystal structure but tend to concentrate at dislocations and grain boundaries. Carbon in steel also forms iron carbide, causing the formation of carbide-ferrite clusters called pearlite which harden and impede dislocation motion. Grain boundaries alter the process of transfer of slip from one grain to another due to their size and misorientation.

Five simultaneous conditions that act together in concert can result in the restriction of plastic deformation and energy absorption in iron: (1) solute atoms which cluster around dislocations and grain boundaries; (2) the presence of iron carbide particles; (3) the myriad number of crystalline grains and their size that make up the actual steel; (4) the contraction of the bcc lattice as the ambient temperature decreases, and (5) the substantial increases in yield strength as temperatures decrease and strain rates increase. The thermal expansion of iron from cryogenic temperatures to ambient temperature virtually mirrors the shape of the ductile-to-brittle sigmoidal curve (see *Figure A4*).

When iron is subject to increases in strain rate, its yield strength also increases. This is due to insufficient availability of thermal activation energy for deformation to occur by slip. Instead, many of the grains fracture by direct cleavage rather than by sliding along the various planes of atomic density that contain dislocations, which decrease yield strength but increase ductility. The yield strength shown in *Figure A1* is determined by a slow strain rate tensile test at 10^{-4} to 10^{-2} strain/sec, whereas the Charpy V-notch (CVN) test is conducted at strain rate of 6.1×10^{2} strain/sec or more, depending on the height of drop. At -70ºC, this higher strain rate will raise the yield strength from 138 MPa (20 ksi) at 20°C to about 485 MPa (70 ksi) (Zerrilli, Armstrong and Arnold, 2009). Below -70ºC, pure iron typically fractures in the Charpy V-notch impact test by cleavage with minimal energy absorption of 5-7 joules or less, whereas the yield strength of iron markedly increases and has virtually no ductility.

The yield strength of iron alloys in compression as a function of temperature, plastic strain and high strain rate is described in the Zerrilli-Armstrong model (1988) for commercially pure iron in the following relationship:

$$\sigma_y (\varepsilon_p, \dot{\varepsilon}_p, T) = \sigma_a + B \exp(-\beta T) + B_0 [\varepsilon_p]^{0.5} \exp(-\alpha T)$$

where
σ_y = yield strength
σ_a = athermal component of yield stress
ε_p, $\dot{\varepsilon}_p$ = plastic strain and strain rate
α, b = material parameters, depending on crystal structure
T = temperature, ^oK
B, B_0 = material constants
$\sigma_a = \sigma_g + k_h / (L)^{0.5} + \varepsilon_p^n$

The athermal component can be described as the internal frictional stress of the crystal structure of bcc metals. The variable σ_g depends on the amount of solutes present and the dislocation density of the iron alloy, k_h is the stress intensity of the microstructure, and L is the average ferrite grain size diameter. The variable ε_p^n is the amount of strain hardening that occurs during plastic deformation. This yield strength-deformation model shows that multiple processes and conditions are simultaneously occurring and how yield strength and deformation of iron alloys are affected at different temperatures and strain rates. The properties of steels are heavily influenced by the presence of alloying elements which can be either beneficial or adversely affect their behavior at different temperatures.

A more simplified equation of the Zerrilli-Armstrong model (Holmquist and Johnson, 1988) for commercially pure iron is:

$$\sigma_y = 65 + 1033\, e^{-(0.00698T + 0.000415T \ln \varepsilon_{sr})} + 266\, \varepsilon_s$$

where
ε_{sr} = strain rate, per sec
ε_s = strain

The coefficient of thermal expansion of iron increases from near absolute zero to ambient temperatures and has the same shape as the ductile-to-brittle energy absorption as shown in *Figure A3*. Not only does the bcc lattice expand, but more thermal energy becomes available for activation for atomic movement to accommodate the deformation which absorbs the applied energy before complete fracture occurs.

Effects of Alloying Elements on the Brittle-to-Ductile Transition of Steel

Commercially pure iron is a reference base by which the impact behavior of steel alloys can be measured and compared to when alloying elements are present. Structural steels are iron-base alloys whose principal alloying elements are carbon, manganese, silicon, chromium, copper, nickel, and molybdenum. Phosphorus and sulfur are generally kept below 0.02% to retain ductility and toughness and to provide isotropic mechanical properties. Micro-alloy additions include aluminum, vanadium, niobium (columbium) and titanium which reduce grain size and can improve yield strength or hardenability if the steels are quenched and tempered. Deoxidizing elements such as silicon, manganese and aluminum are added to combine with interstitial elements like carbon, sulfur, phosphorus, oxygen and nitrogen to improve mechanical properties.

a. *Carbon*. The interstitial element carbon is the most influential alloying addition to steel. As carbon content increases in steels, the shape of the impact energy absorption curve becomes more angular and the point of inflection is not as marked and sharply defined as in pure iron. The shape of the ductile-to-brittle transition curve of carbon or low alloy steels is characterized by certain features as shown in *Figure A2*. These features are designated as the transition temperature, the upper and lower shelf energies, the angularity Θ of the transition zone and the nil-ductility temperature which manifests itself at the temperature of dry ice or other colder cryogenic fluids. At the transition temperature, approximately 50% of the fracture surface is ductile and 50% brittle cleavage. Carbon finds its way into bcc crystal defects by pinning dislocation motion, forming iron carbides in the form of pearlite colonies, filling vacancies and segregating at grain boundaries. All these occurrences tend to decrease impact energy absorption by restricting the absorption mechanisms of iron and the amount of plastic deformation by blocking slip and favoring brittle cleavage fracture. From a carbon range of 0.11% to 0.50%, for every increase of 0.01% C, the transition temperature increases by about 3.1ºC (Rinebolt and Harris, 1951; Burns and Pickering, 1964). Carbon markedly shifts the transition temperature of steel to the right and depresses the position of the upper shelf, as shown in *Figure A2* for several structural carbon steels.

b. *Manganese*. The alloying element manganese has approximately the same atomic diameter as iron, making it substitutionally solid in steel. Manganese decreases the transition temperature of steel and is an essential element in steelmaking compositions for structural steel. The absence of manganese would result in substantial presence of deleterious interstitial sulfur and oxygen. Normal manganese ranges are about 0.4-1.5% for most structural steels. For every

0.01% Mn in this range, the transition temperature is decreased on average by 0.38° to 0.46ºC (Reinbolt and Harris, 1951).

The effect of manganese in typical ranges found in structural steels is shown in *Figure A6*. The transition temperature for steel as a function of % manganese is a linear function. Large percentages of manganese can transform steel alloys from the bcc lattice to the fcc lattice, as found in various high manganese carbon steels and duplex stainless steels.

c. *Phosphorus* is an interstitial element having an atomic radius smaller than that of the iron atom, permitting it to fit into the voids of bcc iron, similar to carbon. Phosphorus tends to segregate at grain boundaries (Bhadesia and Suh, 2015). Phosphorus is usually kept within the range of 0.020-0.040% or less for most structural steels. Exceptions are for bars, screw stock or plates which require higher machinability. Phosphorus is a very potent alloying element which sharply raises the yield strength of ferrite and directly affects the shape of the ductile-to-brittle transition curve. Phosphorus causes an increase in transition temperature by raising it 7º-7.8ºC for every 0.01%, based on several investigations (Reinbolt and Harris, 1951; Hoyt, 1952; Spitzig, 1972). See *Figure A7* for the effect of phosphorus on transition temperature.

d. *Sulfur* is another detrimental interstitial element that markedly decreases energy absorption upon impact. In general, sulfur is kept below 0.030-0.40% in most modern commercial structural steels. For steels requiring very high impact toughness, sulfur is restricted to 0.006% or less. However, reducing the sulfur content to levels as low as 0.001% substantially changes the shape and slope of the transition curve by reducing the theta angle, shown in *Figure A8.* Sulfur does not markedly shift the transition temperature in concentrations found in structural steels when sulfur is restricted to 0.05% or less, as shown in *Figure A9.*

However, the upper shelf energy of steel is considerably reduced by increasing additions of sulfur above 0.006%. The reduction of upper shelf energy when sulfur concentrations are increased above 0.006% becomes an exponential decay function that occurs over an energy range of 120 joules, as shown in *Figure A10*. In the normal range of sulfur found in structural steels, the reduction of upper shelf energy is approximately linear. For every 0.01% increase in sulfur, the energy absorption at the upper shelf decreases by 14 joules, as shown in *Figure A11*.

e. *Silicon* is a deoxidizing element, typically found in structural steels up to 0.40%. However, it has a mixed effect of decreasing the transition temperature. In silicon ranges from 0.04 to 0.18, silicon slightly decreases the transition temperature by 0.22ºC for every 0.01% Si. From 0.19 to 0.40, the normal range for most structural steels, silicon increases the transition temperature by an average of 0.7ºC per every 0.01% Si (Reinbolt and Harris, 1951). The plot of *Figure A12* indicates that increasing silicon up to 2.5% also linearly increases the transition temperature.

f. *Copper and chromium* have minimal effects on the transition temperature of lower carbon structural steels (Hoyt, 1952).

g. *Aluminum* tends to decrease the transition temperature and raises the upper shelf energy, as shown in *Figure A13*. Aluminum is added to the steel melt as a deoxidizer and combines with nitrogen. Aluminum reduces grain size and lowers the transition temperature of killed steels by 1.7ºC for every 0.01% aluminum (Chilton and Roberts, 1980). Aluminum is usually restricted to 0.075% max.

h. *Nickel* is a beneficial element that decreases the transition temperature. The presence of nickel in structural steels is typically found in (a) weathering steels to about 0.80%, (b) steels intended for use in low temperature locations, and (c) quenched and tempered steels used in machinery up to 2.0% for hardenability and toughness. In the range of 0.02 to 0.4%, the transition temperature is decreased by 0.3ºC for every increase of 0.01% nickel (Hoyt, 1952). Higher percentages up to 3% have a diminishing effect in reducing transition temperature, where the reduction is only 0.13ºC for every 0.01% of nickel. This behavior was simplified in the linear plot of *Figure A14*. Steels with more than 5% nickel start to form duplex steels where fcc iron co-exists with bcc iron.

i. *Molybdenum* up to 0.30% generally raises the transition temperature slightly by 1.4ºC for every increase of 0.01% molybdenum (Reinbolt and Harris, 1951), due to formation of molybdenum carbides dispersed in the ferrite matrix. The correlation between transition temperature and molybdenum content is shown in *Figure A15*. Although molybdenum does promote grain refinement, it simultaneously raises yield strength. Because molybdenum also promotes hardenability, it is typically present in several quenched and tempered steels used in applications involving yield strengths greater than 345 MPa [50 ksi].

j. *Niobium (columbium)* in hot rolled steels in the range of 0.045 to 0.68% decreased the transition temperature by 1ºC for every 0.01% Nb (Chilton and Roberts, 1980) due to its effects on the reduction of grain size by pinning austenite grains with niobium carbides. It is more effective in normalized steel due its binding with carbon where it reduced transition temperature by 1.0ºC for every 0.01% Nb. The correlation of transition temperature and % niobium is shown in *Figure A16*.

k. *Vanadium* is a potent grain refining element used in ASTM A572 structural steels. Reducing grain size will also reduce the transition temperature. Vanadium slightly increases transition temperature up to 0.18% vanadium, and then decreases it afterwards up to 0.28% by 1.45ºC for every 0.01% (Vishnevsky and Steigerwald, 1968). This differing behavior was linearized in *Figure A17*. Using ASTM grain size numbers from 4 (coarse) to 10 (very fine), the transition temperature decreases by 12.7ºC for each increase in ASTM grain size number (Petch, 1959). The grain size for commercially hot rolled steels employing the use of aluminum to kill the steel is at least ASTM 5 or finer.

l. *Plate thickness* also has an effect on transition temperature. When plate thickness is reduced through hot working, grain sizes are refined, and larger detrimental silicate and sulfide inclusions are also reduced in size. Based on a thickness range from 13 mm to 40 mm for aluminum or silicon-aluminum killed steels, for every increase in thickness of 1 mm, the average transition temperature increased by 0.9 to 1.1ºC, as shown in *Figure A18* (Shank, 1957). The effect of smaller grain size substantially reducing transition temperature is considerable, as shown in *Figure A19.*

The Shape of the Ductile-to-Brittle Energy Absorption Curve

The general shape of the ductile-to-brittle energy absorption curve with variable carbon contents is shown in *Figure A2*. Components of the sigmoidal curve include an upper shelf energy absorption level, a transition slope angle Θ, and a lower shelf whose energy absorption is typically about 5-9 joules. Interstitial elements carbon, sulfur, phosphorus, nitrogen and oxygen have influential effects on the energy absorption behavior of the ductile-to-brittle transition curve. Phosphorus, nitrogen and oxygen are controlled by deoxidation and their combination with specific alloying elements in a steel heat, resulting in their restriction to tolerable levels. Carbon, phosphorus and sulfur have the strongest effects on the shape of the ductile-to-brittle transition curve and whether the transition temperature either increases of decreases. The shift in transition temperature as a degree of misfit between the atomic radius of iron vs. percentage of that radius by the alloying elements of steel is

shown in *Figure A3.* Where there is substantial misfit, the larger the shift in transition temperature. The interstitials carbon, phosphorus and sulfur have detrimental effects on energy absorption. Phosphorus is particularly adverse in increasing transition temperature. Other elements with atomic radii similar to iron are generally beneficial and often combine with the interstitials.

a. *Estimating Transition Temperature from Composition*

By taking the individual effects of each alloying element on the transition temperature of commercially pure iron, an estimate of the transition temperature can be made. The actual compositions of several commercial alloys, along with their published ductile-to-brittle transition curves where the transition temperature were determined from actual tests, were compared with the estimations of the predictive equations developed in this study.

Steels included in this study were: ASTM A588 Grade 50, A572 Grade 50, A537 Class 1; also, API 5L X65 and ABS EH-36. The following predictive equation includes the effects of niobium and vanadium and plate thickness, but grain size was not made a variable because it is not typically reported commercially. Instead of grain size, section thickness took grain size effects into account. Actual ASTM grain sizes are normally not reported on mill certification sheets provided by steel producers, who routinely describe the steel as manufactured to “fine grain practice”.

Using the various correlations and linear slopes for specific elements obtained from the metallurgical literature, an empirical equation for determination of transition temperature in ºC from the chemical composition and section thickness was developed as follows:

$$T_{CVN} = -70 + 311(\%C) - 53(\%Mn) + 780(\%P) + 74(\%S) + 69(\%Si) - 13(\%Ni) + 12(\%Cu) + 145(\%Mo) - 106(\%V) - 102(\%Nb) - 170\ (\%Al) + 0.9(t - 13)$$

where T_{CVN} = Charpy V-notch transition temperature, ºC

t = thickness, mm

Actual weight percentages of each element were taken from certified heat or product analyses of the steels cited in *Table A1.*

This transition temperature prediction equation was derived from various sources where compositions of the steels were held constant, but specific elements were varied in percentage by weight. Changes in transition temperatures were thereby determined, with emphasis on

determining the 50% ductile-brittle energy values over a complete range of temperatures. Variation of the prediction equation was determined by selecting compositions from various published papers and reports that list the actual steel compositions and display the full CVN energy vs. temperature curves so that the transition temperatures and upper shelves could be directly verified. The predicted transition temperatures were compared to the actual transition temperatures for various structural steels, as summarized in *Table A1*. The developed prediction equation calculated transition temperatures within an accuracy of 1.2° ± 9.0ºC.

Table A1. Comparison of Predicted and Actual Transition Temperatures

Steel	*Predicted Transition Temperature, ºC*	*Actual Transition Temperature, ºC*	*Error*	*Source of Data*
Alloy 12*	10	3	+7	Vishnevsky & Steigerwald
ASTM A36	+20	+8	+12	Fisher, Kaufmann, et. al.
ASTM A588 Gr 50	-28	-34	+6	Ripling & Crosley
ASTM A572 Gr 50	-56	-47	-9	Marine Structural Toughness Data Bank
ASTM A572 Gr 50	-21	-21	0	Ripling & Crosley
ABS EH36	-69	-72	+3	Anderson & Henry
ASTM A508 Cl 3	-18	-11	-9	Verdiere, Parrot, Forget & Frund
API 5L X65	-77	-94	+17	Pluvinage, Cappelle & Azari
ASTM A212 Cl B	0	14	-14	Iskander & Stoller
ASTM A588	-33	-26	-7	Mistry
ASTM HPS 50W	-61	-61	0	Mistry
A572 Gr 50	-13	-21	+8	Kaufmann & Pense

*NOTE: This specialty steel was used to study the effects of nickel and molybdenum on transition temperature but is normally not used in typical structural applications.

Calculation of the transition temperatures of structural steels proposed for a design specification by evaluating their composition is very useful before a particular steel is finally selected. This aids in determining whether the steel is suitable for the service temperatures that the structure will encounter during its lifetime. This does not imply that testing of the as-received steel in advance of construction is unnecessary. The steel selected and delivered must be tested for its CVN energy before construction under the entire range of temperatures that are anticipated during service, especially at the lowest mean anticipated service temperature (LMAST). The statistical determination of the LMAST is covered in the first part of this report.

Effects of Elements on Upper Shelf Energy Absorption

a. Carbon. Carbon not only increases the transition temperature but also depresses the upper shelf. The sharpest decreases in upper shelf energy occur from 0.1 to 0.3% carbon, shown in *Figure A20*. Further increases in carbon content up to 0.80% show a loss of upper shelf energy by exponential decay. In addition to its effect on the upper shelf, the slope angle Ɵ increases with increasing carbon content. As with the upper shelf energy, the most rapid change in the angle Ɵ occurs between 0.10 to 0.30% carbon. The transition angle Ɵ vs. % carbon is also a sigmoidal exponential function.

b. Sulfur. The presence of sulfur has a very strong depressing effect on the upper shelf energy. The high sulfur content (0.069%) of the rivets and plates of the Titanic are ascribed to be the cause of its disastrous sinking as it struck an iceberg in the North Atlantic in 1912 (Foecke, 1998). In contrast, modern commercial steels have generally kept sulfur levels to 0.020 - 0.050% or markedly less for low temperature applications, especially for ship plates operating in colder waters. The manganese content of the steel used for ship plates of the Titanic was only 0.47%, in comparison to modern steels where the Mn / S ratio is 15 or more. The adverse effect of sulfur on the lowering of the upper shelf is essentially linear from 0.01 to 0.06%, the general range for most commercial steels, as shown in *Figure A20*. The adverse effect of sulfur on upper shelf energy tapers off by exponential decay above 0.06% sulfur.

Sulfur also changes the transition slope angle theta which is similar to the sigmoidal behavior of carbon. Minor additions of sulfur also widen the transition curve, but gradually diminish at sulfur levels not normally found in commercial structural steels. Sulfur contents in steel beyond 0.05% are limited to free-machining steels used in smaller diameter screw and bar stock that require high machinability ratings. For higher performance structural steels, sulfur is kept at 0.006% or less to maintain a high upper shelf toughness of 250 joules [185 ft-lbs] or more.

c. Manganese, by virtue of its linkage with sulfur, raises the upper shelf of the transition curve by 11 J for every 1% manganese. Manganese additions do not significantly alter the transition angle in the normal ranges encountered in structural steels.

Predicting the Upper Shelf Energy of the Transition Curve

Using the composition of the selected steel and the effects of carbon and sulfur on the upper shelf energy and transition angle Θ, the shape of the ductile-to-brittle transition temperature can also be approximated. This estimation will provide a quality check of the actual CVN test results at various temperatures of the steel under consideration.

The upper shelf energy for pure iron is at about 310-325 joules. The elements carbon, sulfur and phosphorus have the most influence on changing the position of the upper shelf, whereas silicon has a lesser effect. Elements which decrease the transition temperature typically do not significantly alter the position of the upper shelf. These elements, which include manganese, nickel, chromium, copper and niobium, have relatively mild or neutral effects on upper shelf energy.

a. *Carbon* has a strong effect on the position of the upper shelf. From a wide range of carbon contents from 0.01% up to 0.80%, the upper shelf energy of structural steels decreases as an exponential decay function, as shown in *Figure A20*. The upper shelf energy prediction equation for carbon in steel is $E_{USE} = 3 + 307\ e^{-[(\%C - 0.0194)\ /\ 0.294]}$, where E_{USE} is in joules. Most structural steels, including those used for machinery, have carbon contents limited to 0.40-0.50%.

b. *Sulfur* is particularly deleterious in reducing the energy absorption of the upper shelf. Like carbon, sulfur in the range from 0.006 to 0.14%, also exhibits exponential decay like carbon, but is linear in the normal ranges of structural steels, shown in *Figure A21*. However, in the normal range of structural steels which restrict sulfur to 0.05% max, the curve can be treated as a linear function. The reduction of upper shelf energy in the linear portion of this range of 0.009% to 0.05% sulfur is severe, whereby each 0.01% of sulfur decreases the upper shelf by 14.6 joules. Many producers accordingly restrict sulfur to 0.01% or less in steels specified for service in cold regions to provide high upper shelf energy absorption if the steels will be subject to impact.

c. *Phosphorus* is another deleterious element that decreases the upper shelf energy. Like carbon and sulfur, phosphorus in steel in the range of 0.01% to 0.20%P exhibits an exponential decay function of energy as phosphorus is increased. Higher levels of phosphorus and sulfur above 0.05% are restricted to free-machining steels. Fortunately for most structural steels, phosphorus is restricted to 0.04% max, whereby the linear portion of the exponential decay function can be used to predict the decrease in upper shelf energy. Upper shelf energy vs. phosphorus in

the range of 0.01% to 0.05% can be represented by a linear function, as shown in *Figure A22*. For each 0.01% increase in phosphorus, the upper shelf energy decreases by 4 joules.

d. *Silicon* is a deoxidizing agent that has a relatively mild effect on reduction of upper shelf energy, as shown in *Figure A23*. For a range of silicon up to 2%, the change in upper shelf energy is essentially linear. For every 0.1% increase in silicon content, the upper shelf energy decreases by 3 joules.

e. *Manganese* has a limited effect on raising the upper shelf energy. Substantial additions are needed to raise the upper shelf energy as shown in *Figure A24*.

f. *Copper* is found in structural steels as a residual element where its usual origin is from copper wire found in the scrap charge to an electric furnace. Copper is not a particularly deleterious element with respect to energy absorption. If intentionally added for atmospheric corrosion resistance, it is usually accompanied by nickel additions which increase the solubility of copper in austenite. The effect of copper alone up to 2% in iron-carbon steels on the upper shelf energy, shown in *Figure A25*, is a linear reduction of the upper shelf energy. For 0.1% of copper present in the steel without presence of nickel, the upper shelf energy would decrease by only 2.4 joules.

g. *Molybdenum i*s typically added to increase hardenability of steel and to increase its yield strength. Molybdenum is a carbide former but has a limited effect on the upper shelf energy. Additions of molybdenum up to 0.30% decrease the upper shelf energy in a linear manner, as shown in *Figure A27.* For every 0.01% of molybdenum in structural carbon steels, the upper shelf energy decreases by 0.72 joules.

The upper shelf energy E_{USE} in joules can be estimated by the following predictive equation:

$$E_{USE} = 3 + 307\, e^{-[(\%C - 0.0194)/0.294]} + 11\,(\%Mn) - 1456\,(\%S) - 390\,(\%P) - 30\,(\%Si) - 16\,(\%Cr) - 24\,(\%Cu) - 72\,(\%Mo)$$

The accuracy of this equation was compared to actual upper shelf energies taken from published sources where the entire ductile-to-brittle temperature curve was made available. Comparisons of the predicted vs. the actual known upper shelf energy values derived from Charpy V-notch testing of alloys of known composition are shown in *Table A2.* Based on the comparisons, the equation has an accuracy of -0.6 ± 10.3 joules, which is within -3.1 ± 4.6% of total upper shelf energy.

Table A2. Comparisons of Predicted and Actual Upper Shelf Energies

Steel	*Predicted Upper Shelf Energy, joules*	*Actual Upper Shelf Energy, joules*	*Error*	*% of Actual Energy*	*Source of Data*
ASTM HPS 70W	243	250	-7	-2.8	Mistry
ASTM A36	149	160	+11	-4.1	Fisher, Kaufmann, et. al.
ASTM A572 Grade 50	143	150	-7	-4.7	Marine Structural Toughness Data Bank
ASTM A508 Class 3	183	170	+13	+7.6	Schill, Forget and St. Catherine
ASTM A508 Class 3	152	150	+2	+1.3	Verdiere, Parrot, Forget & Frund
API 5L X65	256	275	-19	-6.9	Pluvinage, Cappelle & Azari
ASTM A36	129	140	-11	-7.9	Iskander & Stoller
ASTM A588 Grade 30	144	150	-6	-4.0	Ripling & Crosley
ASTM A572 Grade 50	145	136	+9	+6.6	Ripling & Crosley

Selected steels should operate near or in the upper shelf zone at the lowest anticipated service temperature. The ordering of steel with a specific composition may not be practical due to a variety of factors, including availability, price and delivery time. The proposed equations that predict transition temperature and upper shelf energy are useful, permitting the user to determine if the steel, based on heat or product analyses, is suitable for the structure in question and its location. Steels with very low levels of sulfur, carbon and phosphorus can be ordered at additional cost. Structure that are commonly impacted or have sustained fatigue cracking and operates at sub-freezing temperatures, the safety and long term service of the structure takes precedence over or cost and acquisition time.

Correlation of Charpy V-Notch Impact Energy with Plane-Strain Fracture Toughness

After much experimental work, many prior investigators (Corten and Sailors, 1971; Roberts and Newton, 1981; Barsom and Rolfe, 1987) found direct correlations of Charpy V-notch impact test values with the slower strain rate plane-strain fracture toughness test which measures the fracture tolerance of cracked steel members under stress. The critical value of fracture toughness of a material under tensile or bending stress which would precipitate rapid fracture is designated as K_{Ic} or K_{mat}.

Fracture toughness K_{Ic} of a steel is expressed by the general relationship $K = C\,\sigma\,[\pi a]^{0.5}$, where C is a factor of loading geometry, a is the crack length and σ is the stress applied to the remaining section. The cost of testing for plane-strain fracture toughness is about four times that of a CVN impact test, which requires smaller samples and is easily tested at subzero temperatures. The fracture toughness specimen is larger and must meet certain geometric requirements and must be pre-cracked. Charpy V-notch specimens must reflect the section of the plate or component where fracture toughness may be at a minimum, including center sections of thick members. Thinner plates may have smaller grain sizes and lower transition temperatures, in contrast to thicker plates with greater transition temperatures but increased lower shelf energies. There are several other equations which correlate fracture toughness with Charpy impact V-notch toughness, as now listed in *Table A3*.

Table A3. Additional Impact Toughness Correlations to Fracture Toughness

Portion of Energy Absorption Curve	*Equation*	*Energy Range, Joules (ft-lbs)*	*Yield Strength Range, MPa (ksi)*
Transition[A]	$K_{IC}^2 = [0.22(CVN)^{1.5}] \times E$	4 - 82 (3 - 60)	270 -1700 (39 - 247)
Transition	$K_{mat} = [12(CVN - 20)^{0.5}(25/B)^{0.25}] + 20$	4 - 82 (3 - 60)	270 -1700 (39 - 247)
Upper Shelf	$(K_{IC}/y_s)^2 = 5\,(CVN / y_s - 0.05)$	31 -121 (23 - 89)	760 -1700 (110 - 247)
Upper Shelf	$K_{mat} = 0.54CVN + 55$	>60 (44)	<480 (70)
Upper Shelf	$(K_{mat})^2 = \frac{E\,[0.53(USE)^{1.28}]\,(0.2^{U^*})}{1000(1 - v^2)}$ $U^* = 0.133(USE)^{0.256}$	100 - 240[B] (74 - 177)	171 - 985[C] (25 - 143)

[A]This equation is recommended for evaluation of older structural steels with higher sulfur levels already in use.
[B]Based on SINTAP, 1998 and [C]International Institute of Welding, 2013, data ranges for the upper shelf correlations.

NOTE: In the above formulas, "USE" is the upper shelf energy value in joules; "CVN" is in joules; *v* is Poisson's ratio; for steel $v \approx 0.3$; B = thickness in mm; y_s = yield strength in MPa; K_{Ic} and K_{mat} are in MPa $[m]^{0.5}$.

Lowest Mean Anticipated Service Temperature and Acceptance of Steels

The geographic location determines the service temperatures in which the structure operates. These temperatures can widely vary, particularly where winter temperatures are continually below freezing for several months. It is at these temperatures where structural steels are most vulnerable to losses in both impact and fracture toughness.

In the United States and Canada, both large and medium sized airports keep daily records of temperature fluctuations. Due to their proliferation, use of their records provide a reasonable accuracy of the daily colder temperatures when these airports are in the general vicinity of the structure. This report concentrates on structures within the State of Illinois. The methodology presented here to determine the lowest mean anticipated service temperature (LMAST) can apply to any city or regional airport in any state or country.

The intent is that the LMAST should be greater than the transition temperature as determined by the prediction equation which is based on the composition of the steel. The CVN energy of the structural steel should be preferably in the upper shelf region. If the steel is not in the upper shelf at the LMAST, but is in the transition region, its fracture toughness can still be predicted by any of the previously cited equations. Because of the variability of CVN data, an actual energy absorption transition test should be conducted to verify the predicted transition temperature and upper shelf energy. The fracture toughness as determined should be at least sufficient to provide longevity, durability or survivability of the structure if cracked or impacted at the lowest anticipated service temperatures. When there is uncertainty or the fracture toughness as determined is unacceptable, the steel should be tested to evaluate its actual toughness as a function of temperature. If the steel is unacceptable, it should be rejected outright and a search for steels with better impact properties at lower temperatures should be started.

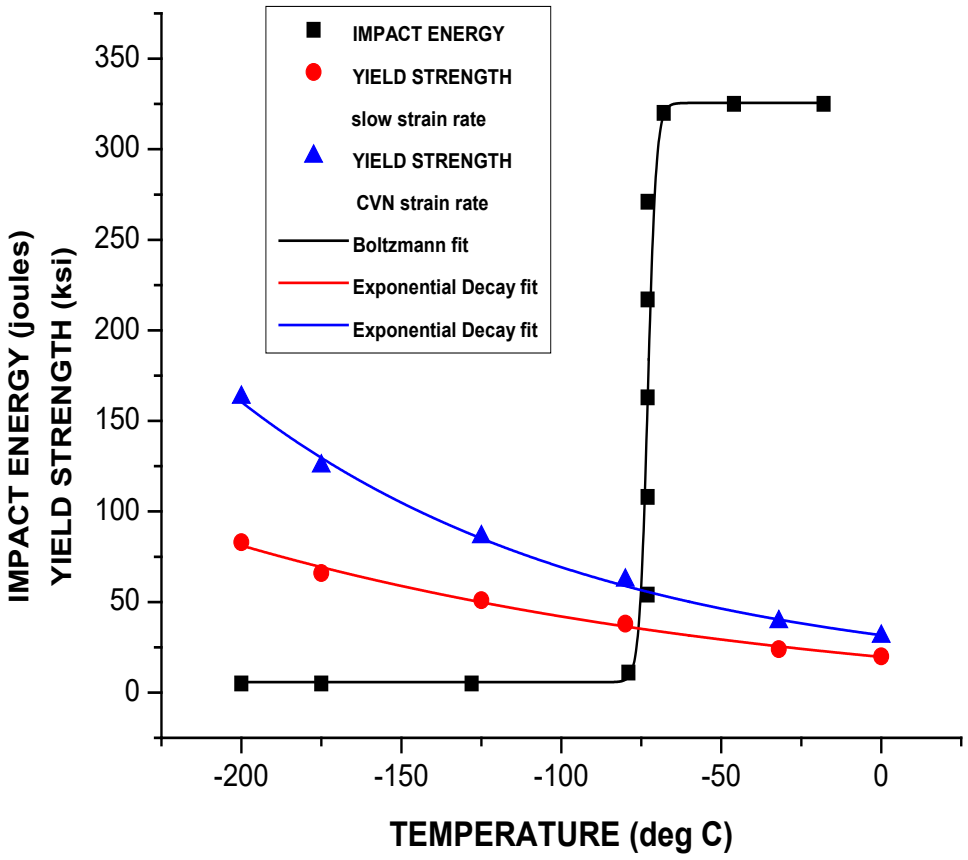

Figure A1. The impact energy absorption of commercially pure iron compared to its yield strength at a range of temperatures. As temperatures decrease, the yield strength of iron at slow strain rates increases, but substantially increases at higher strain rates. The approximate temperature of the lower shelf for commercially pure iron is -70°C, which contains 0.01% carbon. The transition temperature for very high purity iron is approximately -70°C. The impact energy absorption for iron as a function of temperature is a Boltzmann sigmoidal fit and its yield strength at cryogenic temperatures is an exponential decay.

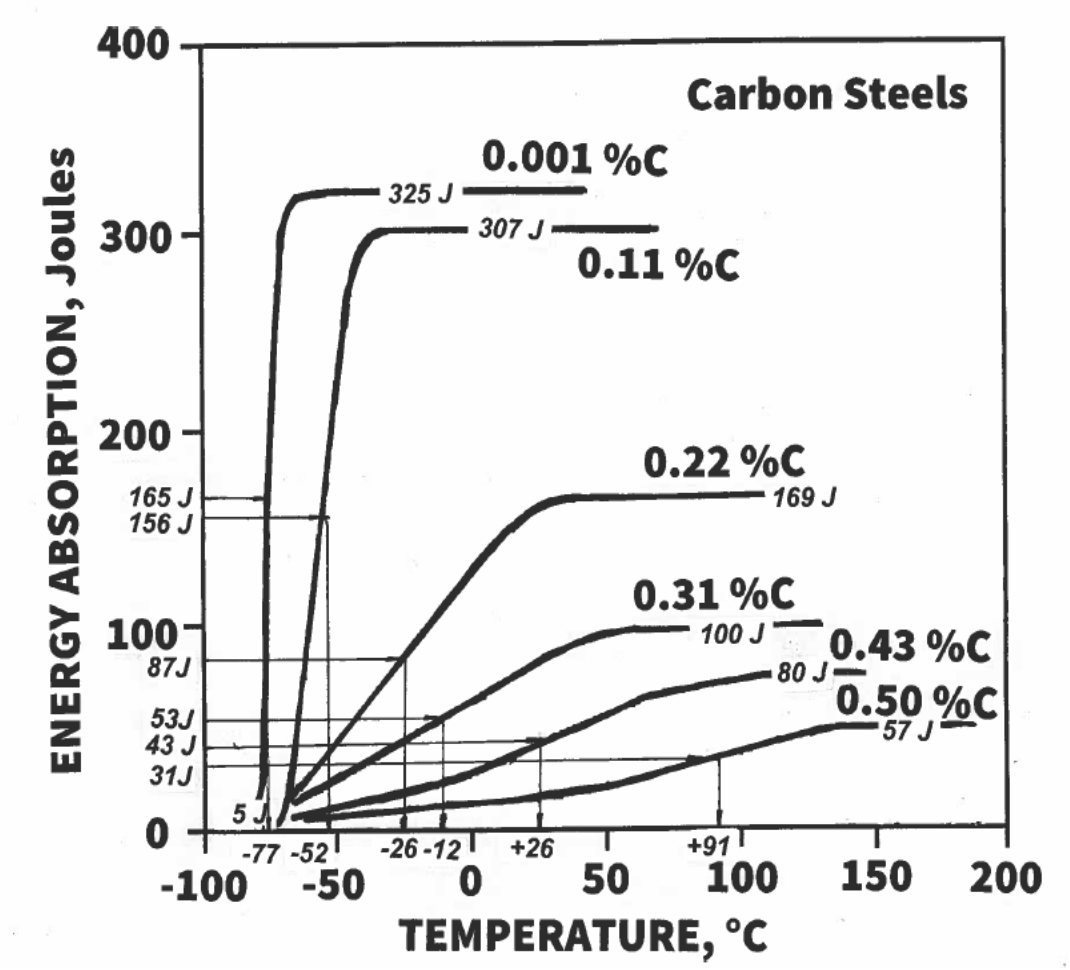

Figure A2. This is a generic plot of the energy absorption vs. temperature for various carbon steels as a function of carbon content. The transition temperature is determined by plotting the upper shelf and lower shelf energies of the tested steel and all test values in between on the ordinate and their respective test temperatures on the abscissa. The average of the [upper shelf energy + lower shelf energy] ÷ 2 is calculated and extended to where the average energy intersects the plotted curve. That point of curve intersection with average energy corresponds to the transition temperature on the abscissa. Because various elements like manganese, nickel, carbon, sulfur and phosphorus can significantly affect transition temperature, this diagram is not intended to represent transition temperatures for all carbon and alloy steels in general. Each steel must be tested due to inherent compositional differences.

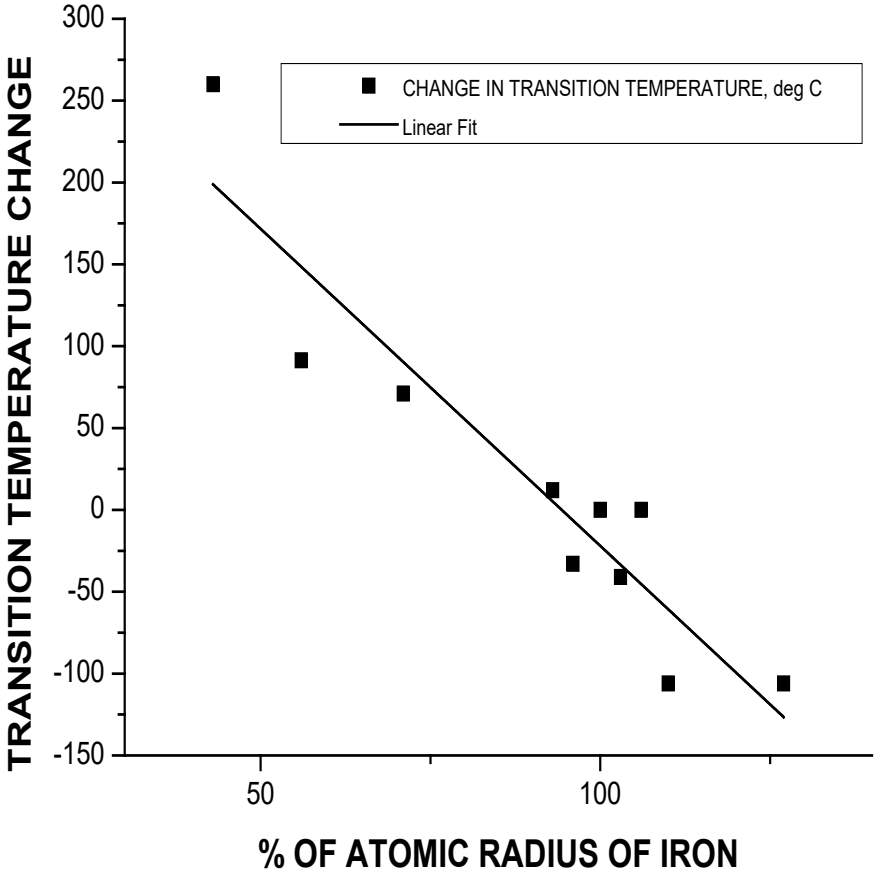

Figure A3. The change in transition temperature is related to the size of the atomic radius of the alloying or residual elements compared to the atomic radius of iron. This is consistent with the fact that interstitials generally raise the transition temperature, whereas most substitutional solid elements in iron decrease or are neutral with respect to the transition temperature. In this graph, the change in transition temperature was based on 1% of the element in iron. However, phosphorus was excluded because 0.12% is the phosphorus limit for free-machining grades.

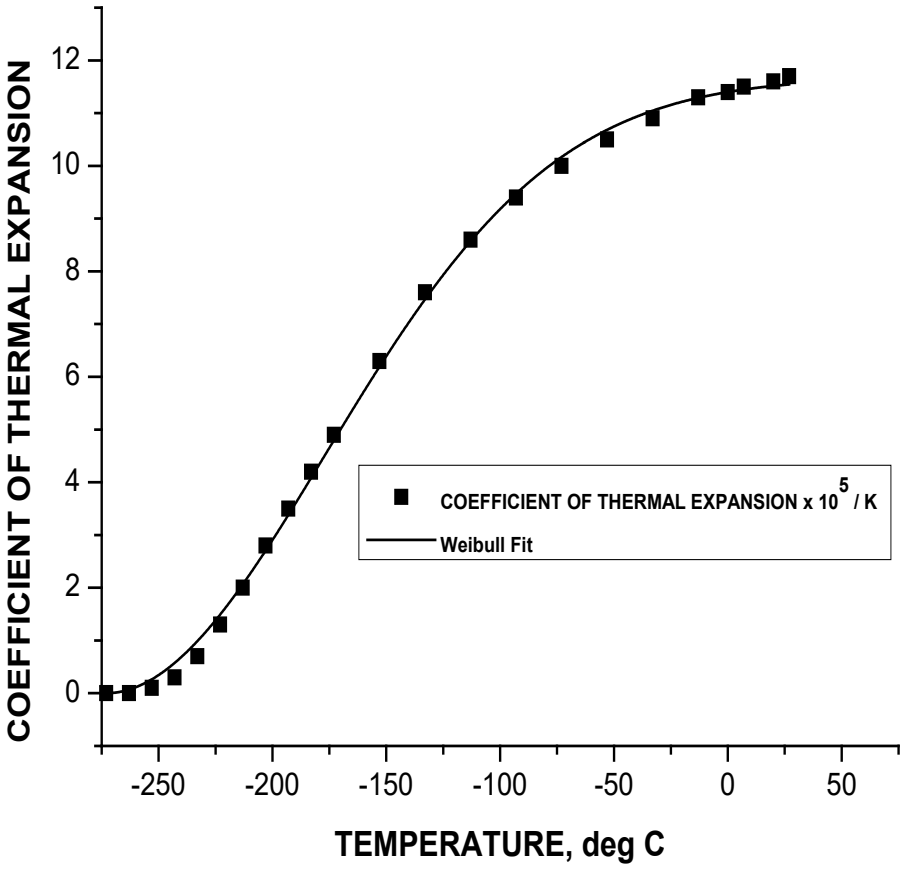

Figure A4. The coefficient of thermal expansion for iron directly corresponds with the brittle-to-ductile transition behavior of body-centered cubic commercial iron and steel alloys. The thermal expansion of iron expands the contracted lattice to permit additional energy absorption and motion of interstitials which restrain a rigidized lattice at lower temperatures. Taken from NBS Monograph 29, 1961.

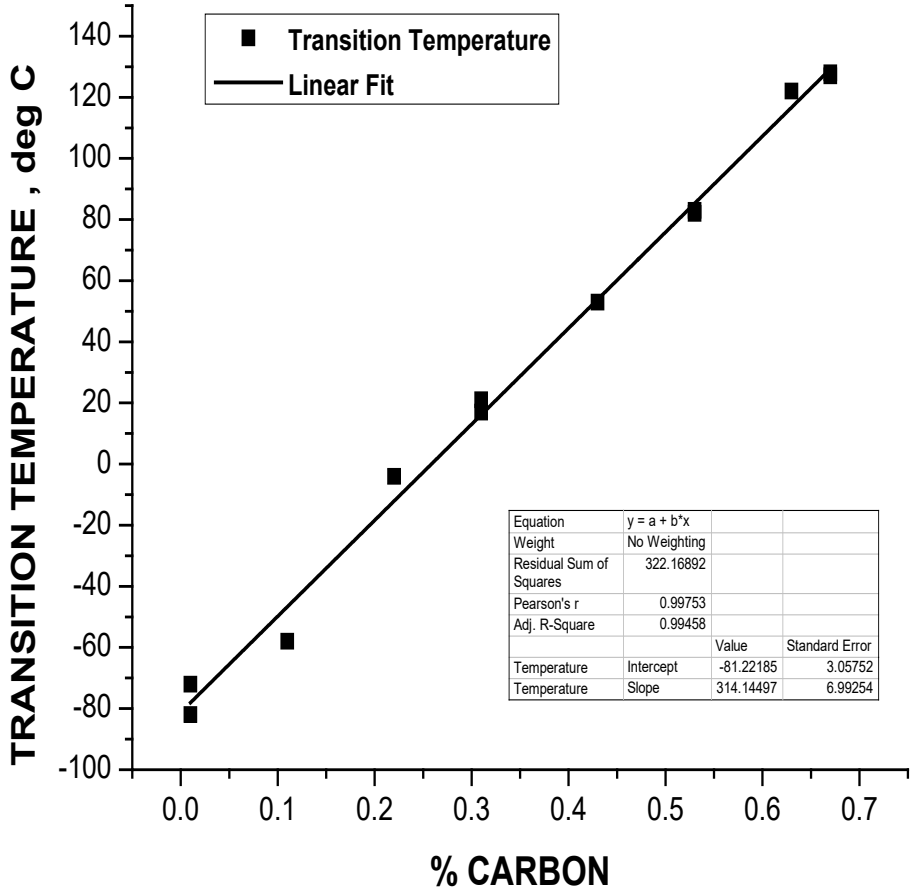

Figure A5. The change in transition temperature for carbon in iron is a linear function with a positive slope of 341. The intercept of this line at -81°C for "zero carbon" is close to the actual location of the sharp transition temperature -70 to -75°C for commercially pure iron.

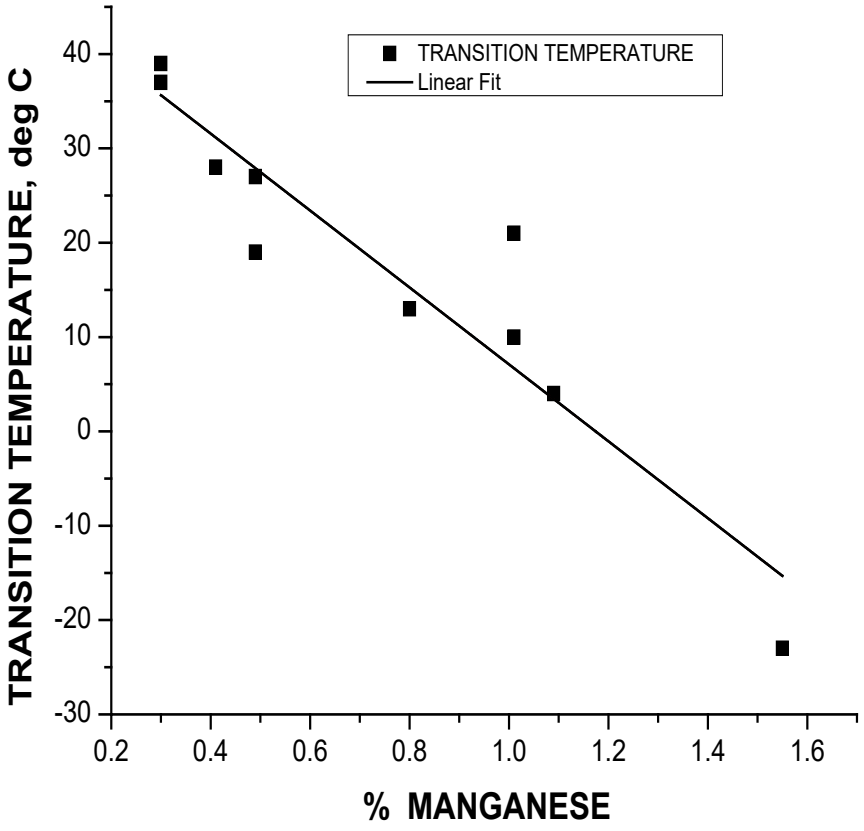

Figure A6. Manganese when added to steel decreases the transition temperature and is strongly correlated in linear fashion (r = -0.934), with a standard error of 5.5°C. Range shown here is typical of most commercial structural steels. Manganese is a deoxidizer that also binds with sulfur, a detrimental element which increases transition temperature and depresses the upper she

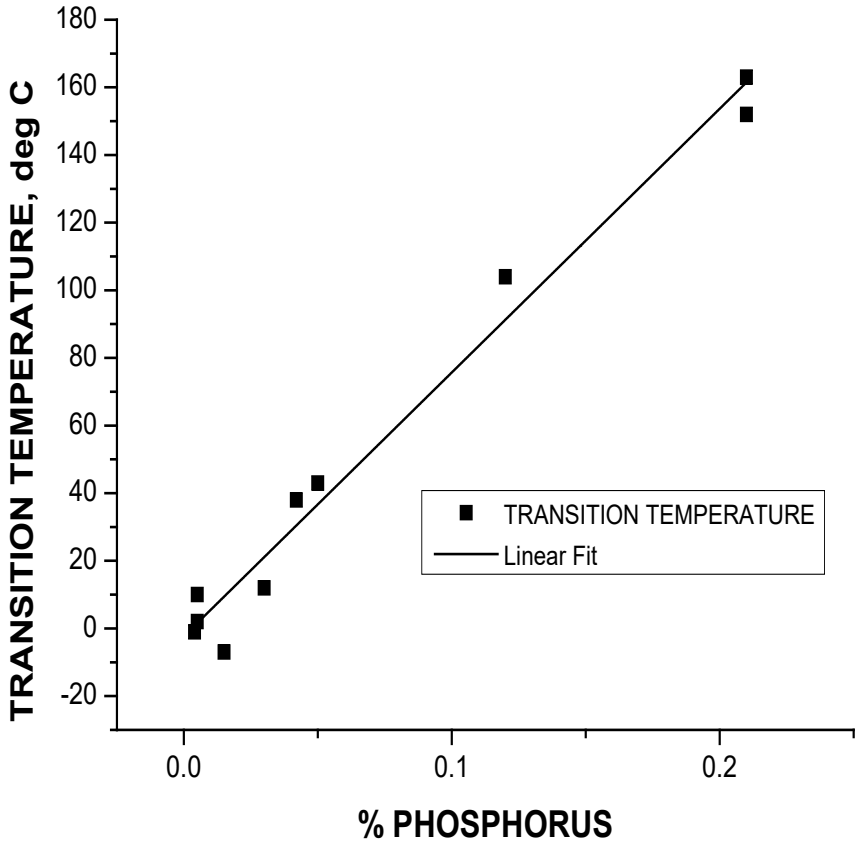

Figure A7. Phosphorus is a potent element that markedly raises the transition temperature linearly with high correlation (r = 0.990). Over the range of concentrations used in structural and free-machining steels, phosphorus can raise the transition temperature by 170°C from very low concentrations in very tough steels up to 0.20% phosphorus used in free-machining grades. Increasing phosphorus concentrations in steel will raise yield strength and machinability but comes as a sacrifice of impact toughness.

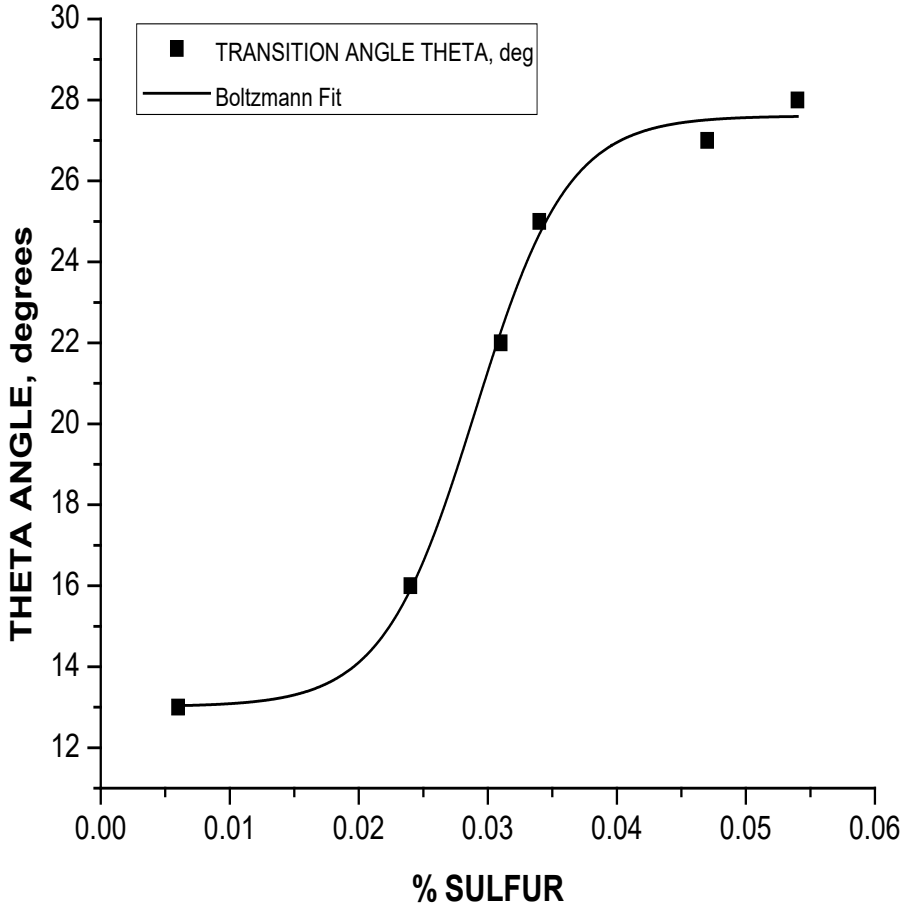

Figure A8. The transition angle theta increases in sigmoidal fashion when sulfur is added to steel. This increase in sulfur content results in an increase in transition temperature and depresses the upper shelf. The shape of the curve mirrors the transition temperature of iron and its various alloys.

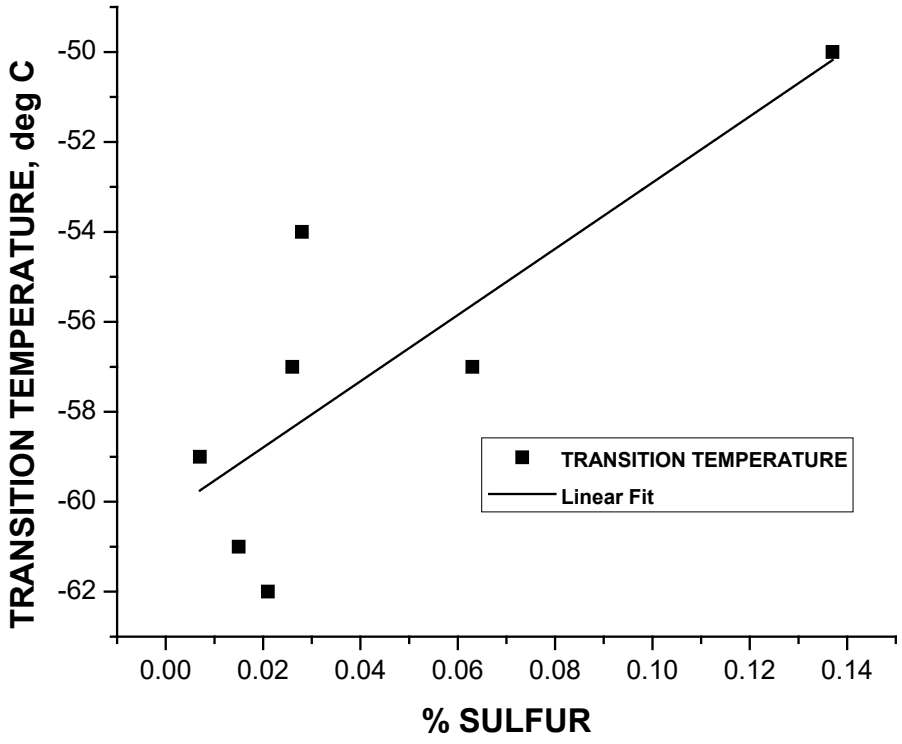

Figure A9. The presence of sulfur in low concentrations can appreciably decrease transition temperature. The linear increase in transition temperature has only fair correlation (r = 0.805). At free machining levels, sulfur is detrimental to impact energy absorption in steels, particularly with respect to upper shelf energy.

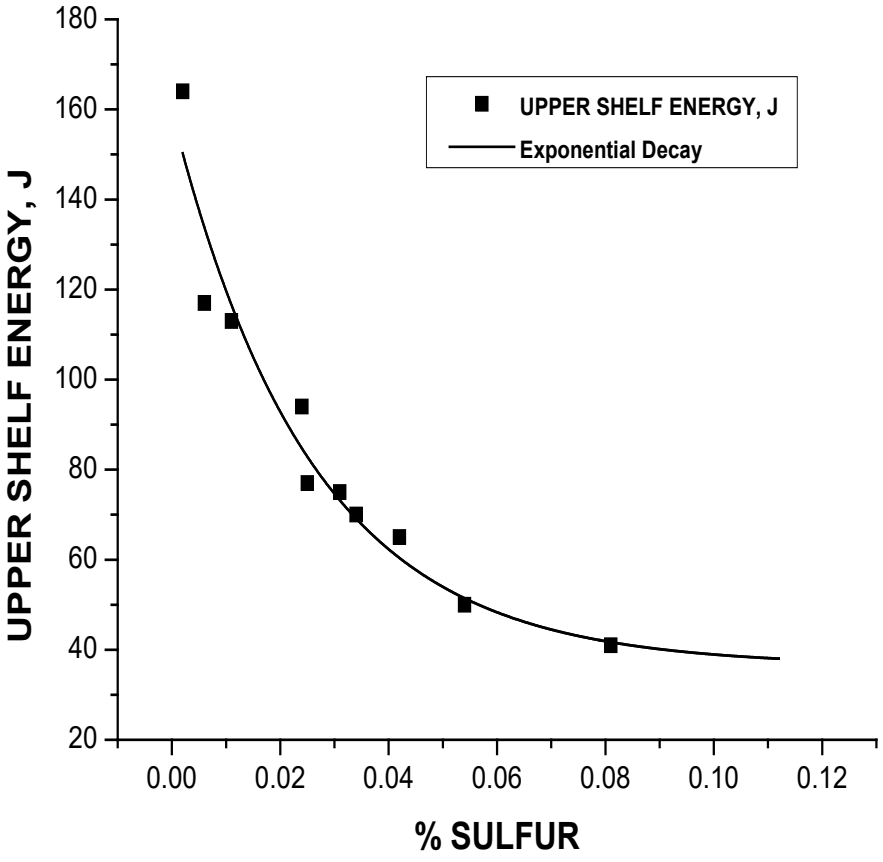

Figure A10. In the full range of sulfur additions to steel, the upper shelf energy is an exponential decay function. At very low concentrations of sulfur below 0.006%, the upper shelf energy can often approach the capacity of Charpy V-notch pendulum impact energy test machines.

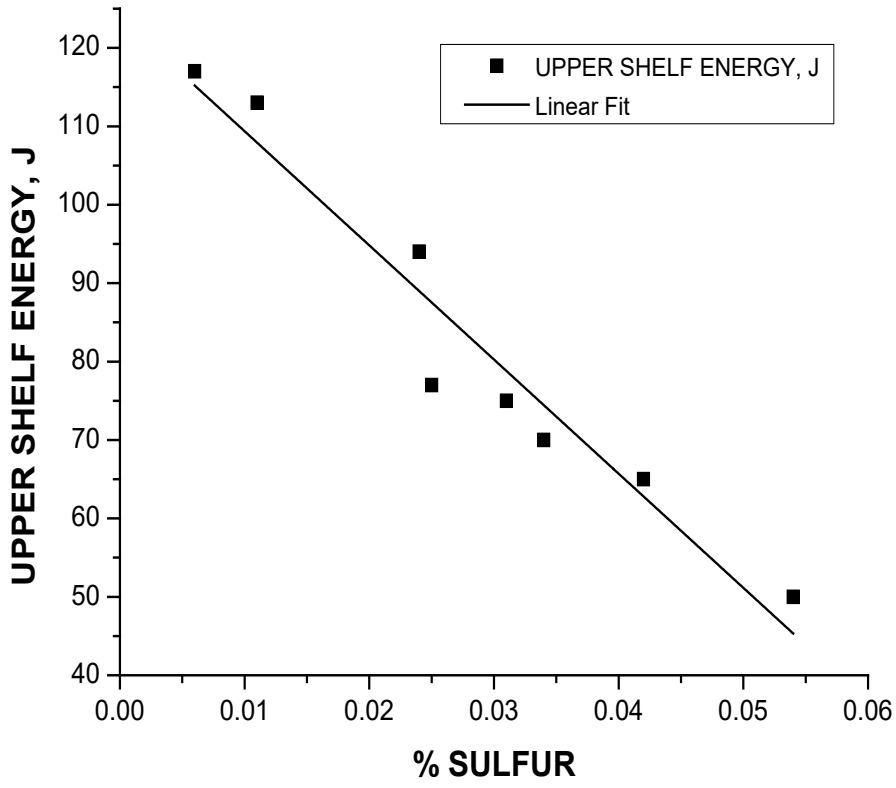

Figure A11. Sulfur has a potent linear effect on depressing the upper shelf energy in the 0.006% to 0.05% range found in most commercial structural steels.

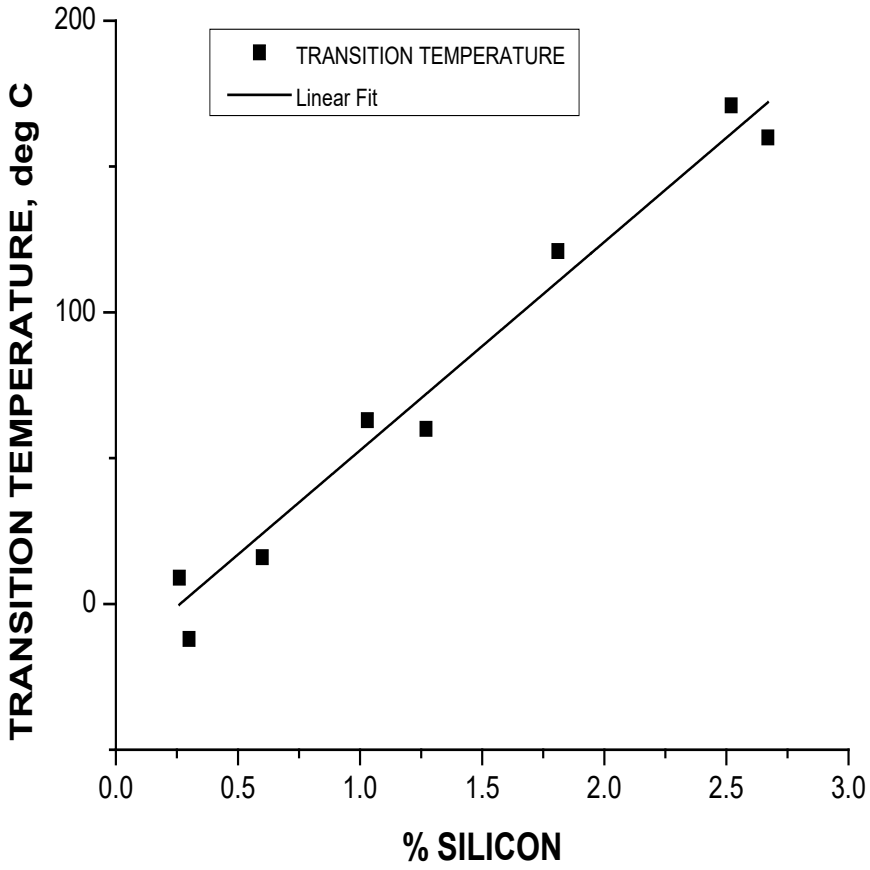

Figure A12. In the normal ranges of silicon for structural steels, transition temperatures increase linearly with increasing silicon content. The correlation is high at r = 0.987, with a slope of +69 and a standard error of ± 4.46°C.

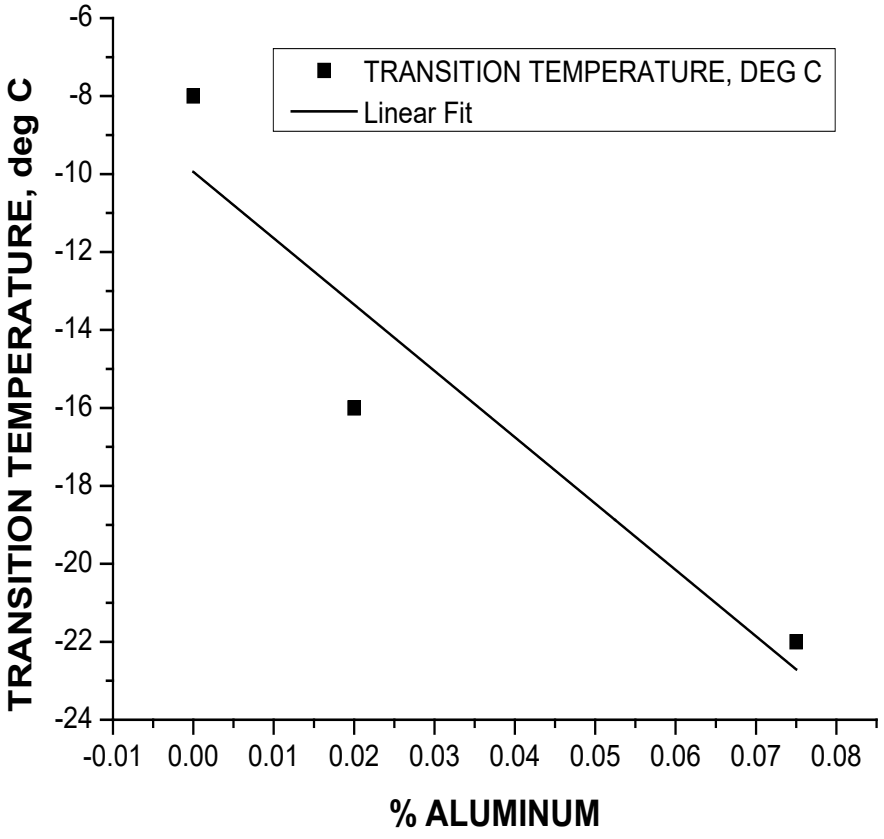

Figure A13. Aluminum is added to killed steels and is typically associated with fine grain practice. Although the number of data points is limited, the addition of aluminum to molten steel decreases transition temperature, with a correlation of r = -0.941.

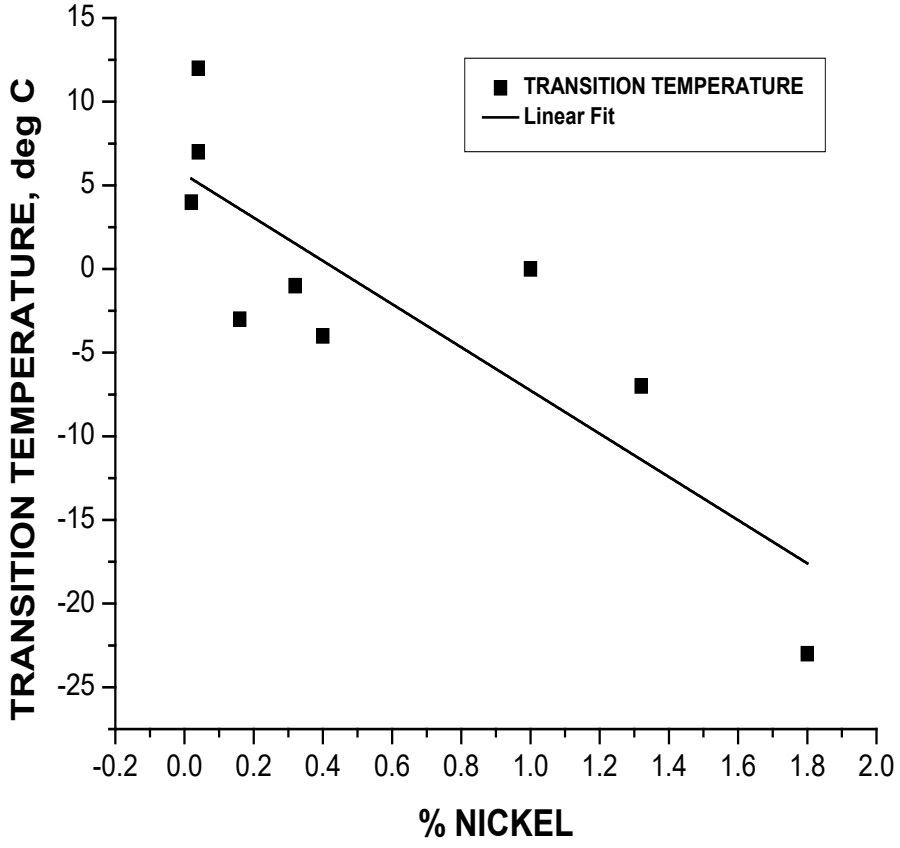

Figure A14. The addition of nickel to alloy steels decreases transition temperature. Correlation is good at r = -0.846 with a slope of -13. However, additions of 1% or more are needed for substantial decreases in transition temperature. Due to its cost, nickel additions to alloy steels are generally reserved for applications in cold regions and low temperature service.

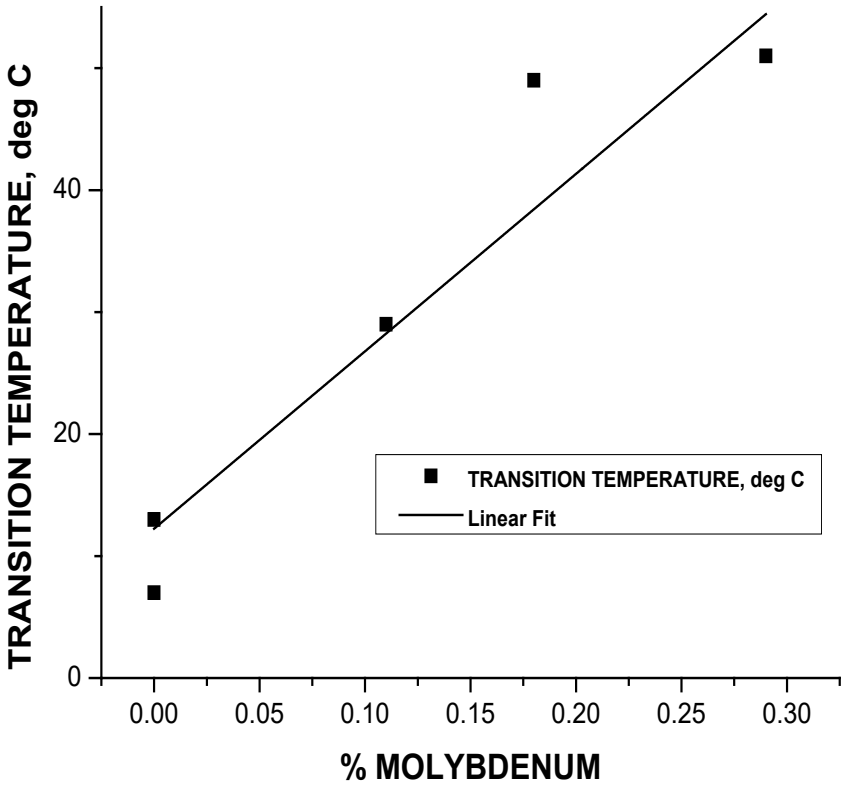

Figure A15. The addition of molybdenum increases transition temperature in linear fashion. The correlation is very good at r = 0.958 with a slope of +145. Due to its ability to form carbides and other hardened precipitates, molybdenum is a hardening agent but has detrimental effects on transition temperature.

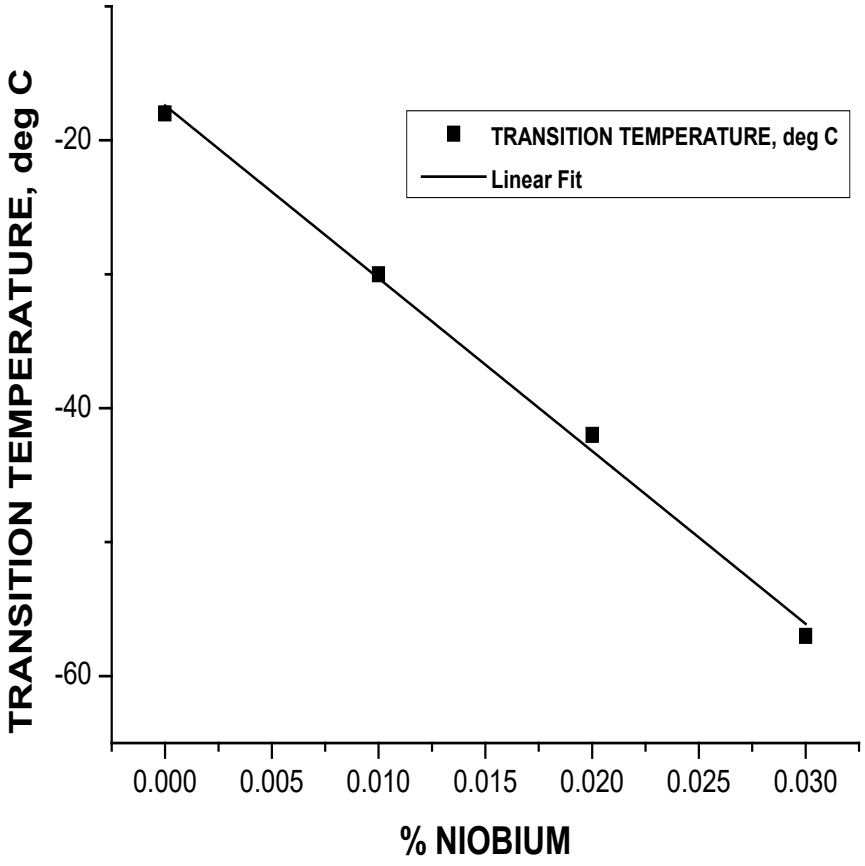

Figure A16. Niobium (columbium) has a beneficial effect on reducing transition temperature. The linear reduction of transition temperature attributed to niobium additions is strongly correlated at r = 0.998.

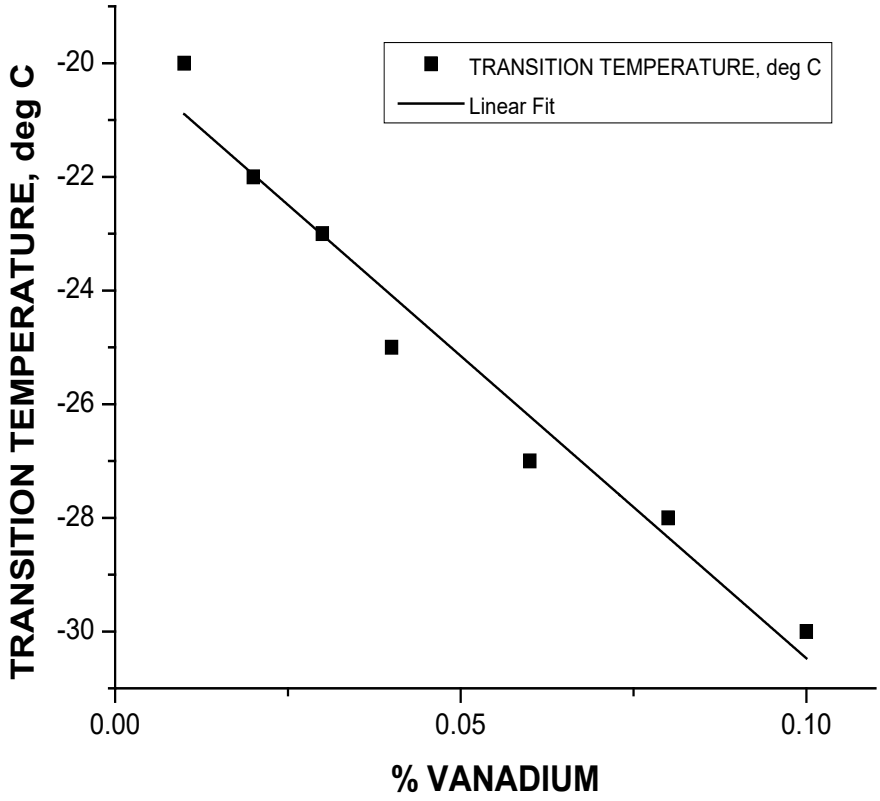

Figure A17. Vanadium substantially reduces the transition temperature in the ranges normally found in structural steels. The linear relationship is well correlated at r = 0.983 with a minimal standard error.

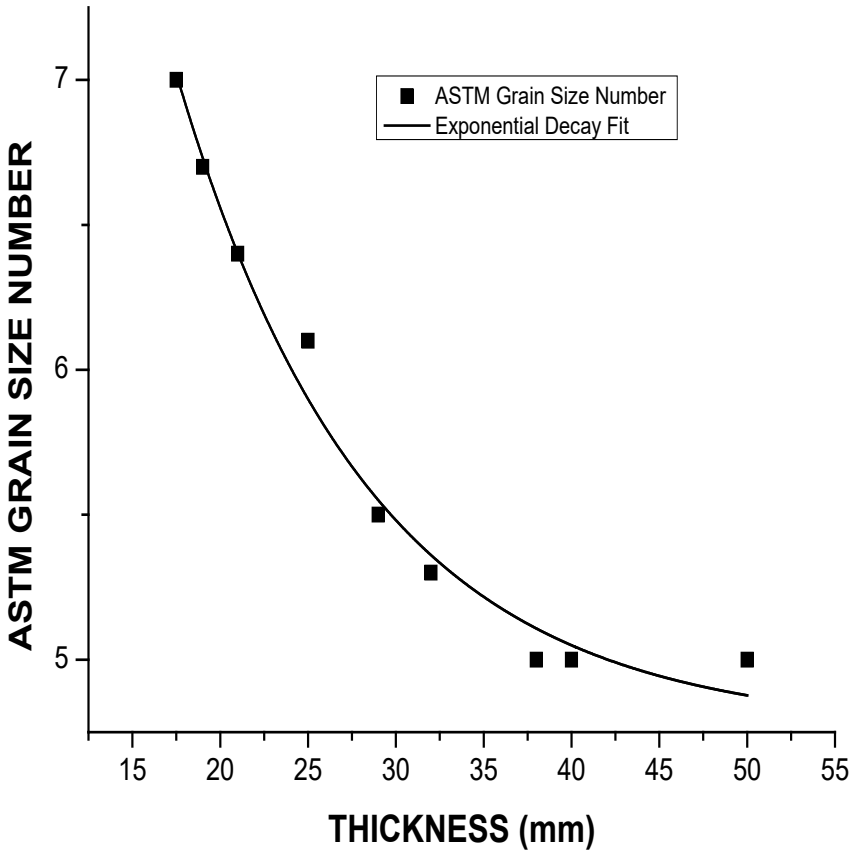

Figure A18. By reducing the thickness of slabs and billets into plates during hot working operations, their grain size is considerably reduced in terms of ASTM grain size numbers, which are inversely related to actual grain size fineness. Reduction in grain size decreases transition temperature, as shown in the following *Figure A19*.

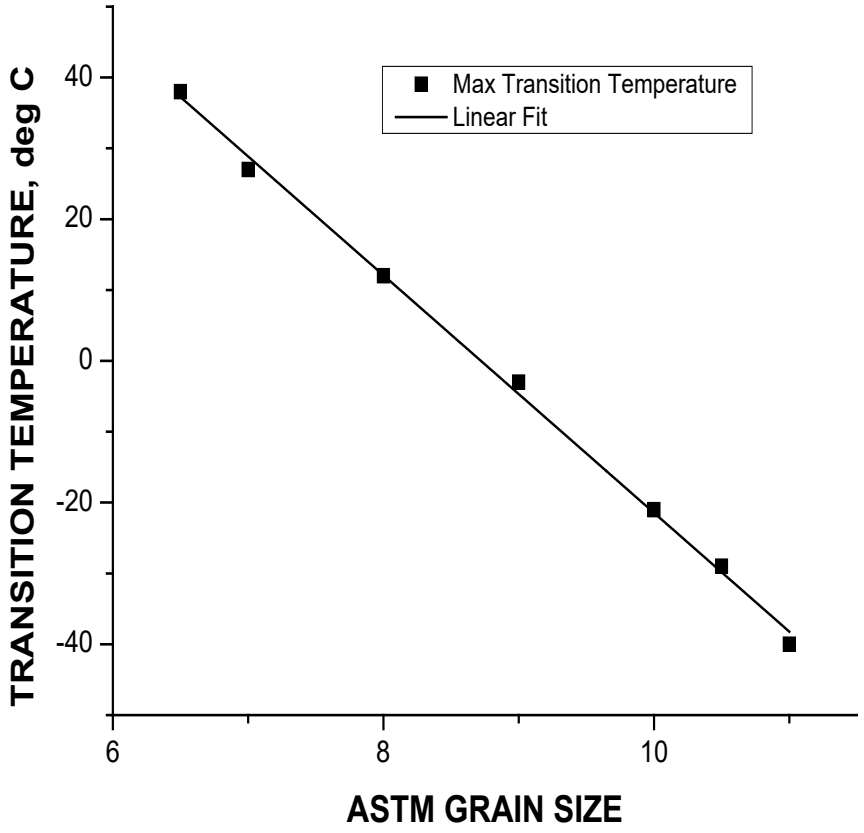

Figure A19. Reducing grain size also reduces transition temperature and is linearly related to ASTM Grain Size numbers with very high correlation at r = 0.999. As ASTM Grain Size numbers increase, the finer the grain size. Elements that reduce grain size and thickness reduction in structural plates during hot rolling practices can confer substantial benefits that decrease the transition temperature.

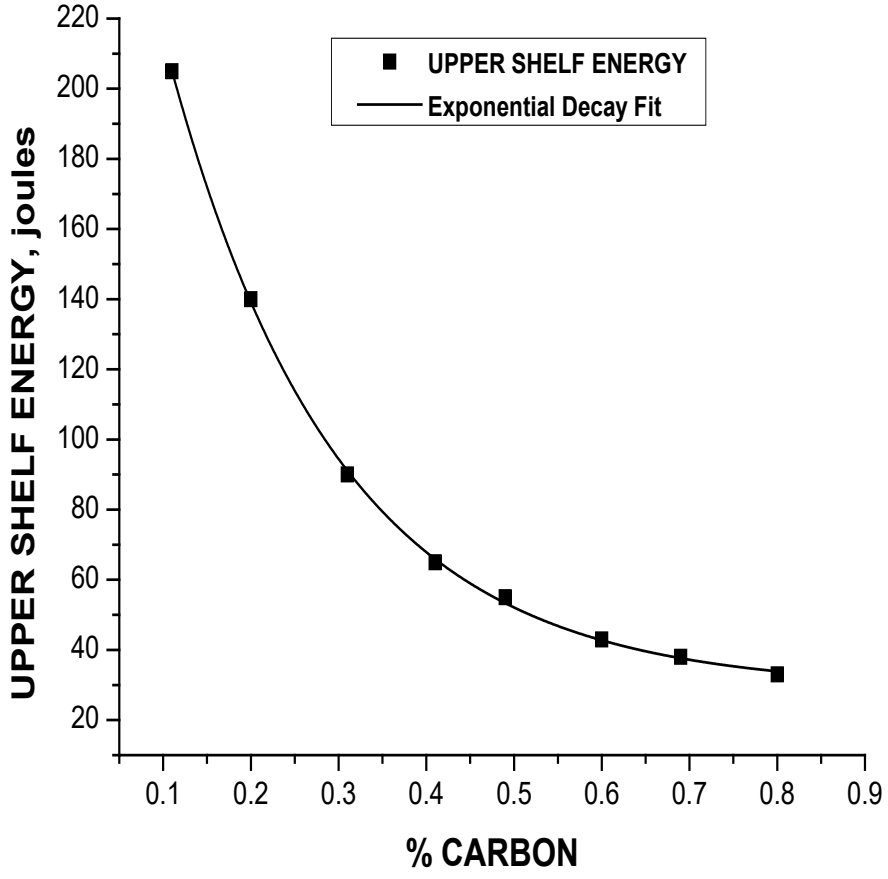

Figure A20. The upper shelf energy is depressed as % of carbon is increased in steel. Upper shelf energy vs. % carbon is an exponential decay function $E_{USE} = 3 + 307\ e^{-[(\%C - 0.0194) / 0.294]}$, where the Charpy V-notch value of upper shelf energy is in joules. This relationship is well correlated at $r^2 = 0.934$.

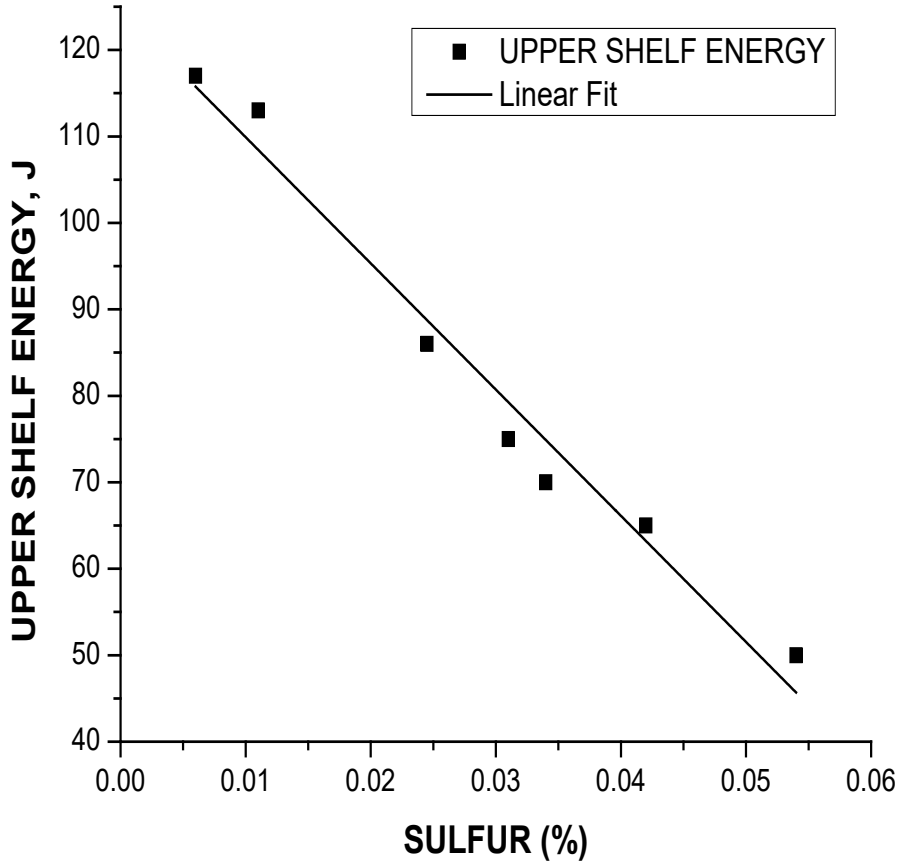

Figure A21. The upper shelf energy of steel is sharply depressed by the addition of sulfur. The range depicted here is typical permitted for sulfur permitted in structural steels. The upper shelf energy vs. sulfur content is linear and sharply negative in this range and is very well correlated at r = -0.987

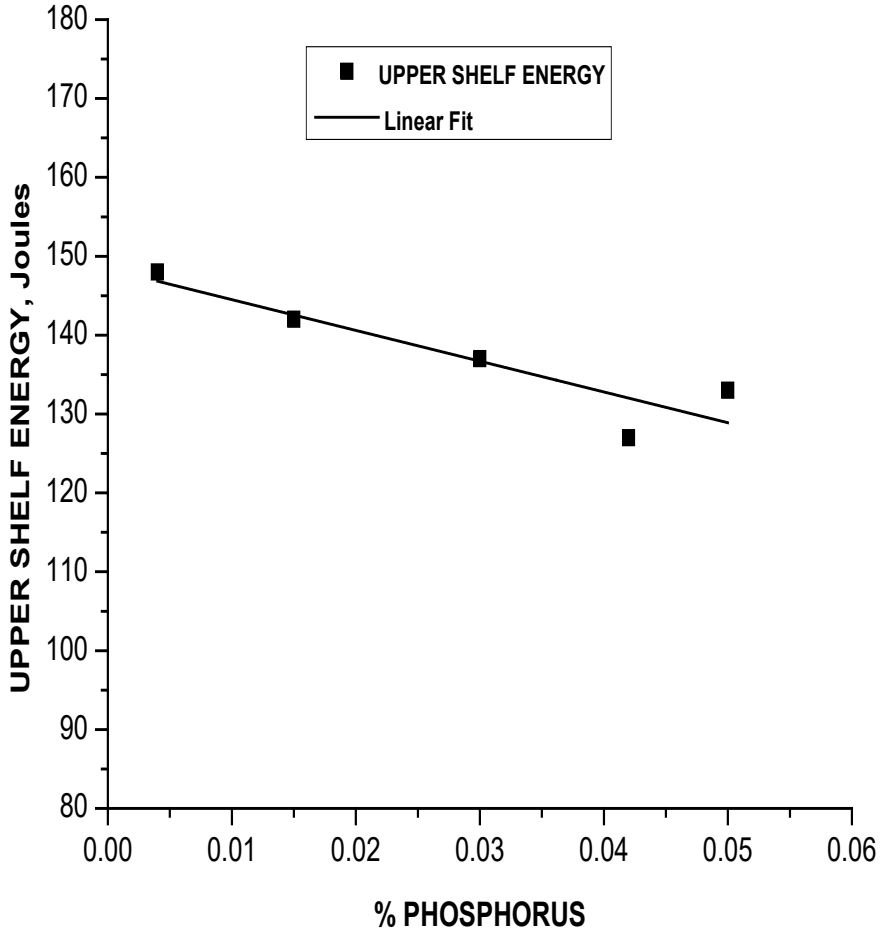

Figure A22. Increasing phosphorus content in steel depresses the upper shelf energy. In the ranges for most structural steels, not including the free-machining grades, the depression is a linear function with good correlation at r = -0.912.

.

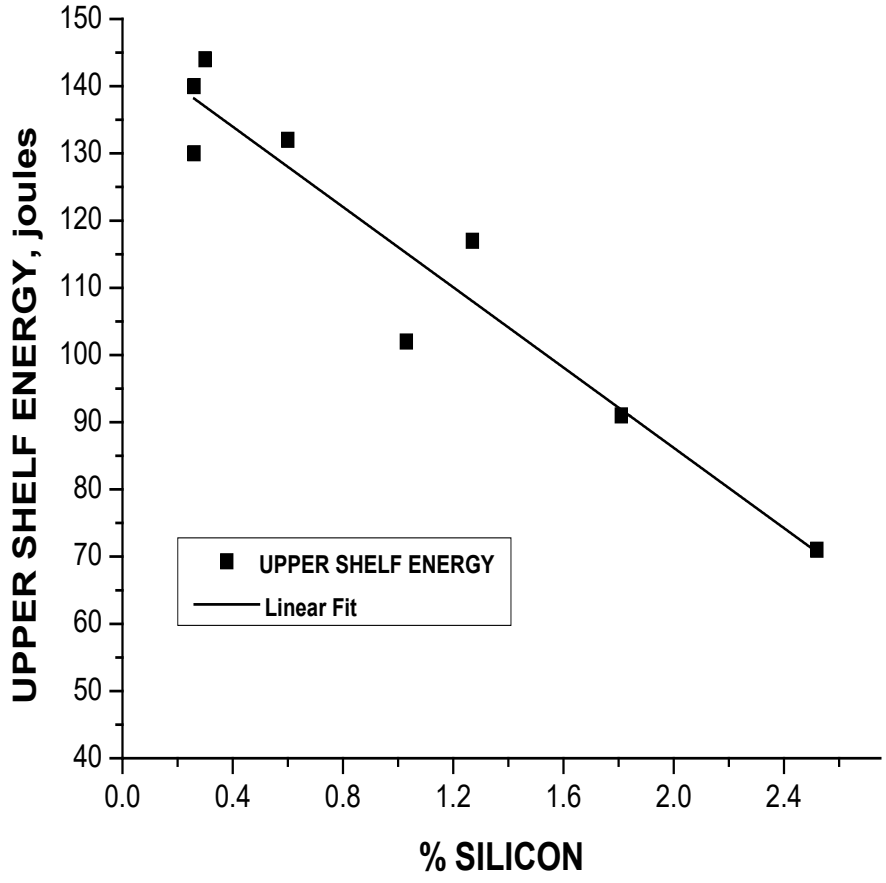

Figure A23. Increasing silicon in steels depresses the upper shelf energy in linear fashion for the typical ranges found in structural steels. The negative correlation is good at r = -0.823

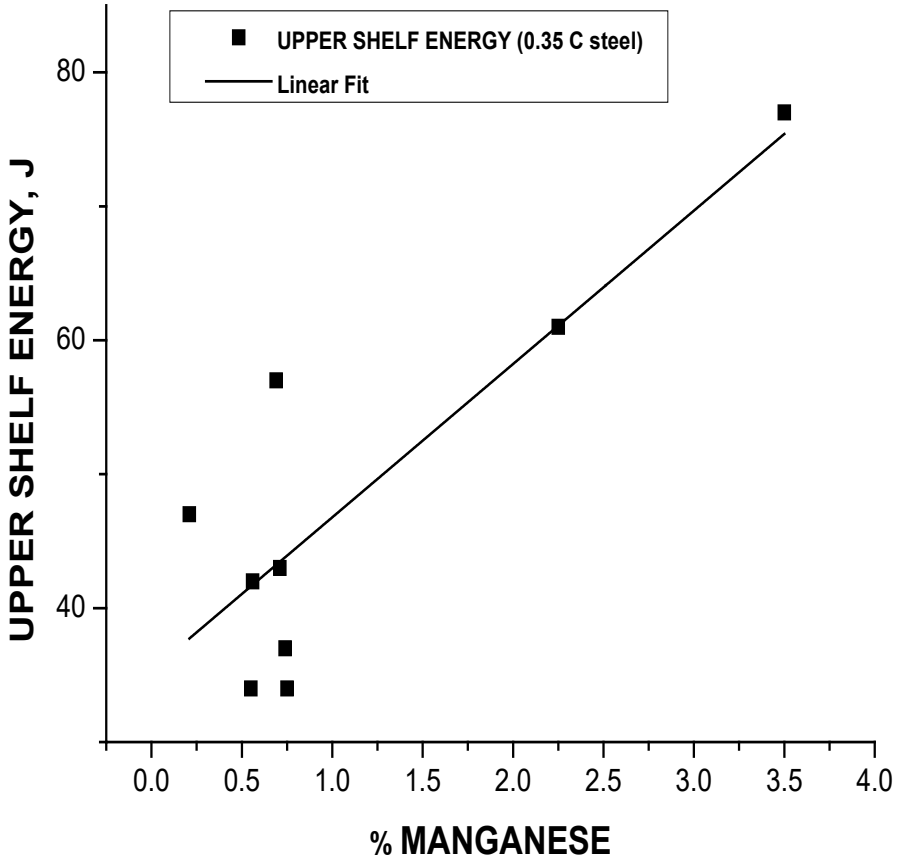

Figure A24. Manganese has a moderate effect on raising the upper shelf energy. Manganese raises the upper shelf at lower carbon contents but mildly depresses the upper shelf at higher carbon contents. There is considerable scatter for steels at higher Mn + C contents and correlation is weak.

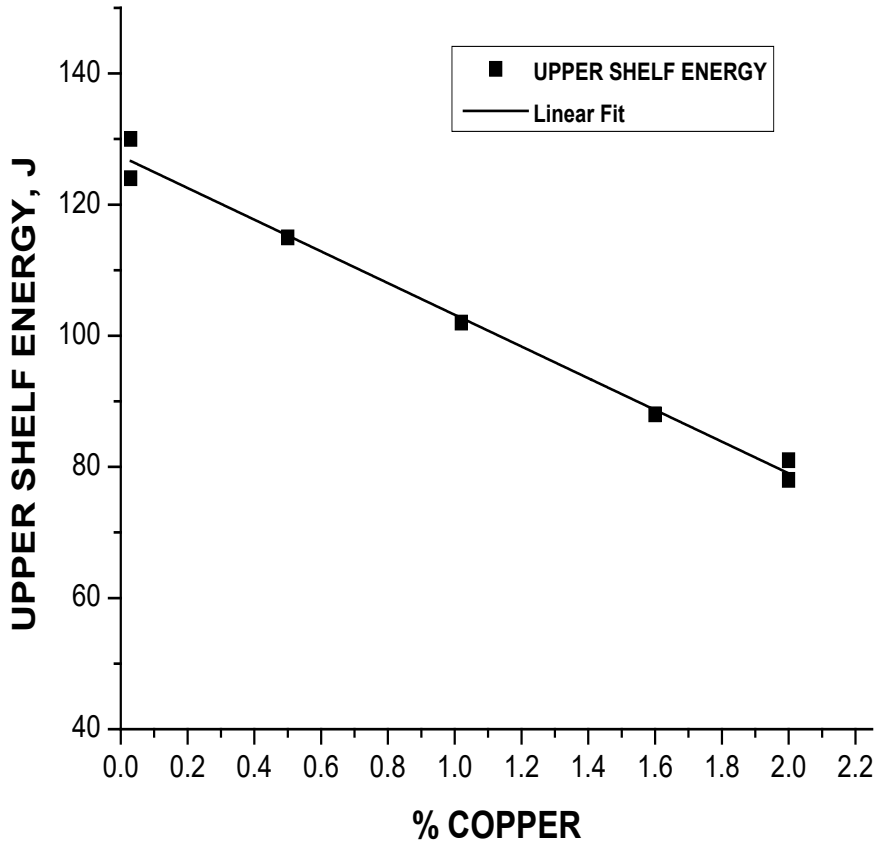

Figure A25. Increasing copper content in steel will depress the upper shelf energy if not accompanied by addition of nickel in the melt. This graph does not include the effects of the presence of nickel when copper is present, which is generally derived from scrap residuals. Nickel increases the solubility of copper in austenite at a minimum of %Ni = 0.5 x %Cu, permitting it to coherently precipitate in the ferrite matrix rather than segregate where “hot shortness” can occur.

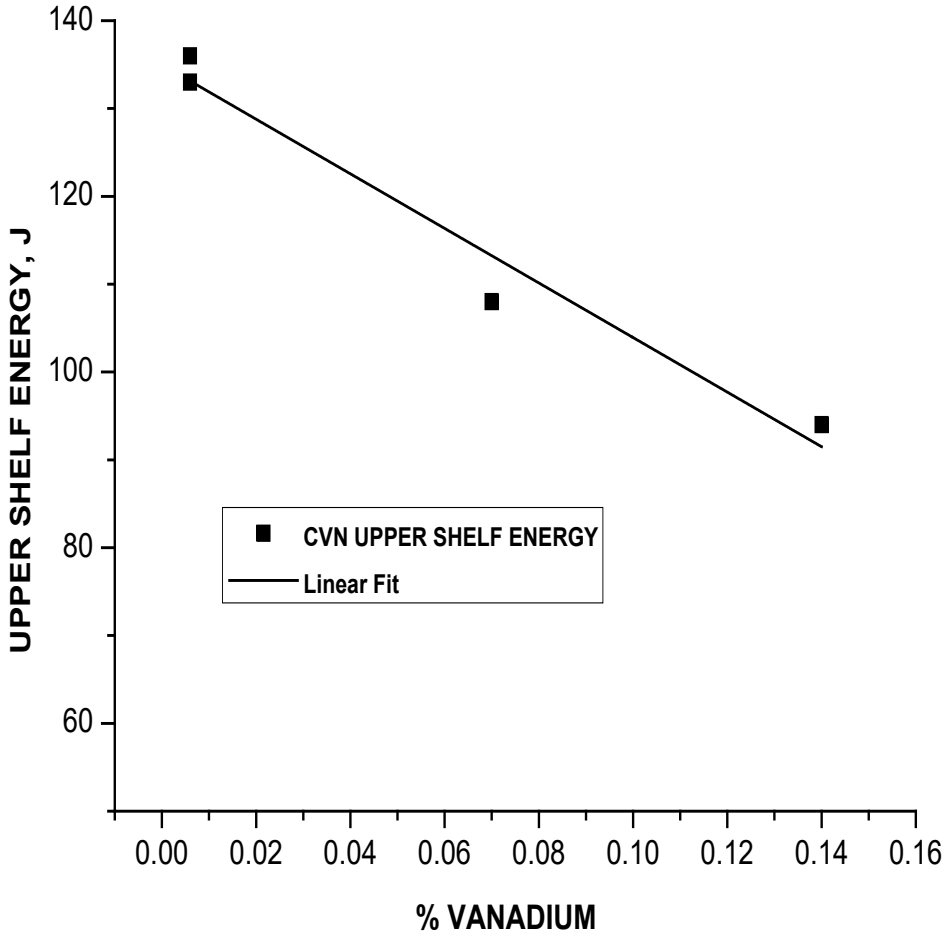

Figure A26. Vanadium additions linearly decrease the upper shelf energy in steels. Vanadium is a carbide and nitride former causing impediments to energy absorption, although their formation increases yield and tensile strength. The plot has good correlation at r = -0.983 with a considerably negative slope.

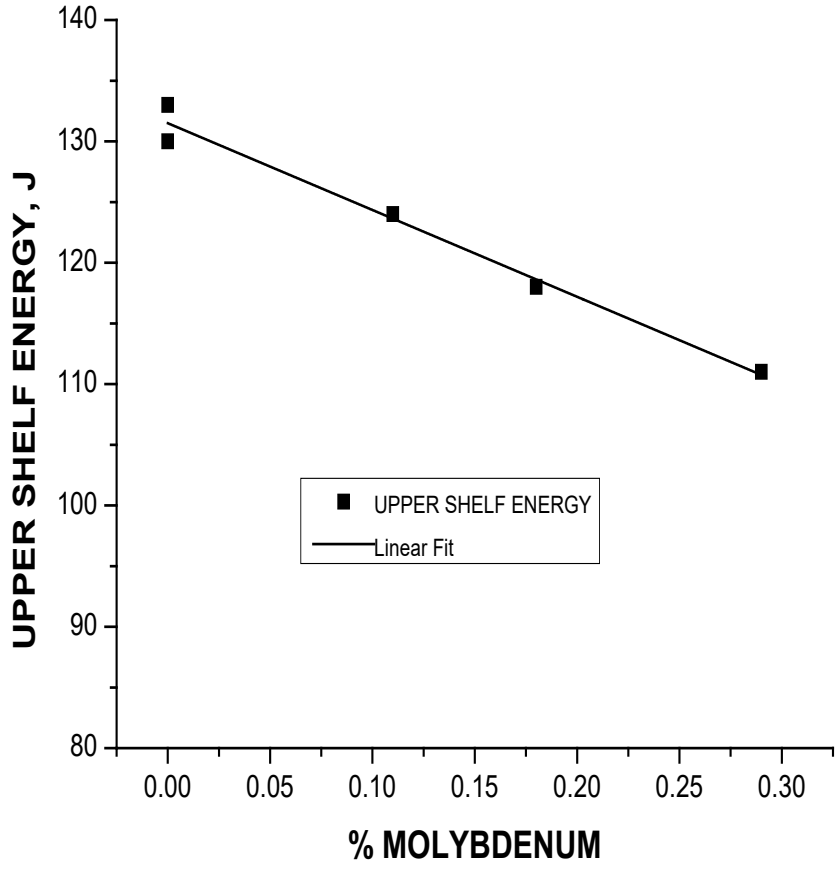

Figure A27. Molybdenum, another carbide former, decreases the upper shelf energy in negative linear fashion as molybdenum concentration increases. The plot of upper shelf energy vs. molybdenum has very good correlation at r = -0.992.

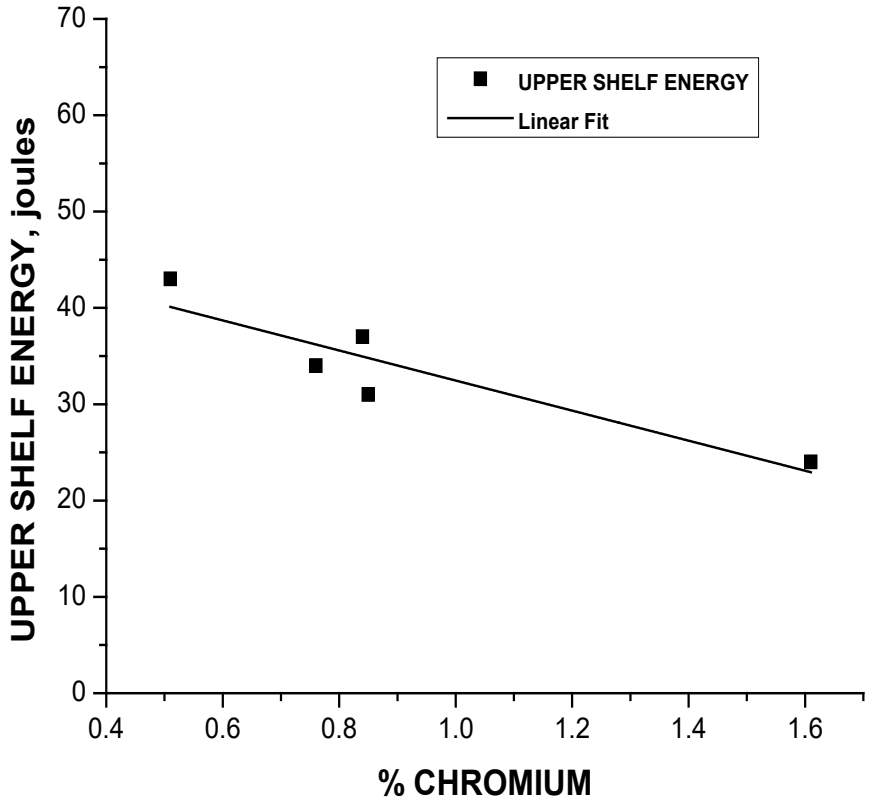

Figure A28. Chromium has a mild linear effect on depressing the upper shelf energy and has good correlation at r = -0.913 with a slope of m = -16.

References

T. Anderson and H. Henry, *Fracture Toughness of Steel Weldments for Arctic Structures*, National Bureau of Standards NBSIR 83-1680, Boulder, CO, Dec. 1982.

D. Andrews and R. Kokes, "Crystal Structure", *Fundamental Chemistry*, Wiley, NY, 1963, p. 262.

J. Barsom and S. Rolfe, *Fracture & Fatigue Control in Structures,* Prentice-Hall, Englewood Cliffs, NJ, 1987, pp 173-176.

H. Bhadesia and D. Suh, "Is a Low Phosphorus Content in Steel a Product Requirement", *Iron and Steelmaking,* Vol. 42, 2015, pp. 259-267.

A. Blake, *Practical Stress Analysis in Engineering Design*, Dekker, NY, 1990, pp 166-167.

K. Burns and F. Pickering, "Deformation and Fracture of Ferrite-Pearlite Structures", *J. of the Iron & Steel Institute, Vol. 202, 1964*, pp 899-906.

J. Chilton and M. Roberts, "Microalloying Effects in Hot-Rolled Low Carbon Steels Finished at High Temperatures", *Metallurgical Transactions*, Vol. 11, 1711-1721, 1980.

R. Corruccini and J. Gniewek, *Thermal Expansion of Technical Solids at Low Temperatures*, NBS Monograph 29, US Dept. of Commerce, Washington, DC, May 1961.

H. Corten and R. Sailors, *Relationship Between Fracture Toughness Using Fracture Mechanics and Transition Temperatures,* T & AM Report 346, University of Illinois, Urbana, 1971.

S. Epstein, "Embrittlement of Hot-Galvanized Structural Steel*", Proceedings of the ASTM, Vol. 32, Part 2, 1932*, pp. 293-379.

J. Fisher, E. Kaufmann, W. Wright, Z. Xi, H. Tjiang, B. Sivakumar and W. Edberg, *Hoan Bridge Forensic Investigation Failure Analysis Final Report*, Wisconsin DOT & FHWA, June 2001.

T. Foecke, *Metallurgy of the RMS Titanic, NIST-IR 6118*, US Dept. of Commerce, Gaithersburg, MD, 1998.

A. Giannattasio, Z. Yao, E. Tarleton and S. Roberts, Brittle-Ductile Transitions in Polycrystalline Metals, *Philosophical Magazine, Vol. 90, No. 30, Oct. 2010*, pp. 3947-3959.

W. Harris and C. Williams, *Report on Metallurgical and Economic Aspects of Ship Steels and Relation to Ship Failures*, National Academy of Sciences, Washington, DC, August,1956.

T. Holmquist and G. Johnson, *Determination of Constitutive Model Constants from Cylinder Impact Tests*, Naval Surface Warfare Center, December 1988.

S. Hoyt, *Metal Data*, Reinhold, NY, 1952, p. 218.

W. Hume-Rothery and G. Raynor, "Imperfections in Crystals", *The Structure of Metals and Alloys*, Institute of Metals, London, 1962, p.363.

S. Iskander & R. Stoller, *CVN Impact Testing of Irradiated Structural Steels Irradiated in a Commercial Reactor,* NUREG/CR-6399/ORNL-6886, Oak Ridge National Laboratory, TN, April 1977.

E. Kaufmann, B. Metrovich and A. Pense, *Characterization of Cyclic Inelastic Strain Behavior on Properties of A572 and A913 Rolled Sections*, ATLSS Center of Lehigh University, Bethlehem, PA, Aug. 2001.

Marine Structural Steel Toughness Data Bank (Abridged Edition), Ship Structure Committee, US Coast Guard, Washington, DC, 1991.

V. Mistry, "High Performance Steel for Highway Bridges", *Proceedings of Advanced Materials for Construction of Bridges, Buildings and Other Structures III, Engineering Conferences International*, 2003.

National Transportation Safety Board, *Collapse of US 35 Highway Bridge, Point Pleasant, WV*, NTSB Report HAR-71-1, Washington, DC, Dec. 1970.

N. Petch, "Ductile-Cleavage Transition in Alpha-Iron", *Fracture*, MIT Technology Press, Cambridge, MA, 1959, pp 54-67.

G. Pluvinage, J. Capelle, Z. Azari and S. Jallais, "Design Based on Ductile-Brittle Transition Temperature for API 5L X65 Steel Used for Dense CO_2 Transport", *J. of Engineering Fracture Mechanics, Vol. 110, Sept. 2013*, pp. 270-280.

R. Reed-Hill, "Vacancies", *Physical Metallurgy Principles,* Van Nostrand Reinhold, NY, 1964, p. 169.

J. Reinbolt and W. Harris, "Effect of Alloying Elements on Notch Toughness of Pearlitic Steels", *Transactions of ASM, Vol 43, 1951,* pp 1175-1214.

E. Ripling, P. Crosley and and R. Armstrong, *Brittle-Ductile Transition of Bridge Steels*, Federal Highway Administration, McLean, VA, Aug. 1989.

R. Roberts and C. Newton, "Interpretative Report on Small-Scale Test Correlation with K_{Ic} Data", *Welding Research Council Bulletin 265, 1-18*, 1981.

R. Schill, P. Forget and C. Catherine, "Correlation Between CVN and Sub-size CVN Test Results for Un-Irradiated Low-Alloy RPV Ferritic Steel", *Materials Science*, February 2013.

M. Shank, "Control of Steel Construction to Avoid Brittle Failure in Structural Steels", *Welding Research Council, NY,1957*, p. 30.

W. Spitzig, "Effects of Phosphorus on the Mechanical Properties of Low-Carbon Iron, *Metallurgical Transactions*, Vol. 3, 1183-1188, 1972.

N. Verdiere, A. Parrot, P. Forget and J. Frund, “Fracture Toughness Determination of a Nuclear Pressure Vessel Steel by Instrumented Charpy Impact Test”, *International Conference on Nuclear Engineering*; Nice, Acropolis (France), Apr 2001.

C. Vishnevsky and E. Steigerwald, “Influence of Alloying Elements on the Toughness of Low-Alloy High Strength Steels”, US Army Materials & Mechanics Research Center, Nov 1968.

R. Wasley, *Stress Wave Propagation in Solids*, Dekker, NY, 1992.

F. Wilson, *High-Velocity Forming of Metals*, Prentice-Hall, Englewood NJ, 1964, pp 6-7.

NOTES